

---

# PREDICTION INTERVALS FOR INTERIM EVENTS IN RANDOMIZED CLINICAL TRIALS WITH TIME-TO-EVENT ENDPOINTS

---

**Edoardo Ratti<sup>1†</sup>, Federico L. Perlino<sup>2</sup>, Stefania Galimberti<sup>1</sup>, Maria G. Valsecchi<sup>1</sup>**

<sup>1</sup>Bicocca Bioinformatics, Biostatistics and Bioimaging Centre B4,  
School of Medicine and Surgery, University of Milano–Bicocca

<sup>2</sup>Department of Statistics, University of Warwick

## ABSTRACT

Time-to-event endpoints are central to evaluate treatment efficacy across many disease areas. Many trial protocols include interim analyses within group-sequential designs that control type I error via spending functions or boundary methods, with operating characteristics determined by the number of looks and the information accrued. Planning interim analyses with time-to-event endpoints is challenging because statistical information depends on the number of observed events, so adequate follow-up to accrue the required events is critical and interim prediction of information at scheduled looks and at the final analysis becomes essential. While several methods have been developed to predict the calendar time required to reach a target number of events, to the best of our knowledge there is no established framework that addresses the prediction of the number of events at a future date with corresponding prediction intervals. Starting from prediction interval approach originally developed in reliability engineering for the number of future component failures, we reformulated and extended it to the context of interim monitoring in clinical trials. This adaptation yields a general framework for event-count prediction intervals in the clinical setting, taking the patient as the unit of analysis and accommodating a range of parametric survival models, patient-level covariates, staggered entry and possible dependence between entry dates and loss to follow-up. Prediction intervals are obtained in a frequentist framework from a bootstrap estimator of the conditional distribution of future events. The performance of the proposed approach is investigated via simulation studies and illustrated by analyzing a real-world phase III trial in childhood acute lymphoblastic leukaemia.

**Keywords** Interim Analysis, Event-driven trials, Prediction Interval, Parametric Bootstrap, Survival Extrapolation

## 1 Introduction

Time-to-event endpoints are often used for evaluating treatment efficacy in many disease areas. However, designing trials in which the primary endpoint is a time-to-event variable is challenging. In this context, the statistical information of interest depends on the number of events that occur rather than on the number of patients enrolled. Accordingly, the trial is usually powered on the expected number of events (Wu, 2018). Interim analyses are increasingly planned to allow early stopping for efficacy or futility for ethical and economic reasons (Wassmer & Brannath, 2025). Group-sequential designs are typically adopted and type-I error is controlled via alpha-spending or boundary methods (Jennison & Turnbull, 2025). The operating characteristics of a group sequential test - power, error rates, and stopping probabilities - depend on the number and timing of looks, on the information accrued at each analysis and on the maximum planned information at the final analysis. Consequently, the protocol must ensure sufficient follow-up to achieve the target number of events required to preserve the nominal power. In addition, interim analyses should be conducted at the information levels specified at the design stage. If analyses are performed at times corresponding to a different number of events than planned, the Type I error probability may be adversely affected (K. K. G. Lan & Demets, 1989) (Proschan et al., 1992).

---

<sup>0†</sup> Correspondence: e.ratti9@campus.unimib.it

However, achieving both aims is difficult in practice. Sample size calculation relies on the correct specification of the survival distribution, yet trustworthy informations on survival estimates are often unavailable at the design stage and may shift as data mature. When the design assumptions prove inaccurate while the trial is ongoing, the operational characteristics of the study could be jeopardize. Since information accrues when events occur, an unforeseen slowdown in event rates can shift interim analyses to information times that depart from the protocol plan or push completion well beyond the planned timeline. This has an impact on the budget and logistics of the trial, even when the nominal power of the trial is preserved. On the other hand, an unexpected increase in event rates may put the trial at risk of being over-run (Whitehead, 1992) and appropriate methods should be considered (Baldi et al., 2020). A disciplined interim monitoring framework can identify such discrepancies early and support timely corrective actions.

In light of these challenges, it is important to prospectively predict while the trial is ongoing the information expected at each planned interim analysis, the maximum (final) information at the scheduled final analysis or the calendar time at which these targets will be reached. If a *maximum-information* approach is adopted, the trial ends once the target number of events has accrued (Kim, 2014). A natural predictand is therefore the calendar time required to reach that target, often termed milestone or time to endpoint maturation (Ou et al., 2019) (L. Wang et al., 2022). In a *maximum-duration* approach, follow-up is limited by a fixed calendar time (Kim, 2014). In this case, natural predictands are the cumulative number of events or, equivalently, the additional number of events expected by future calendar dates and at the planned study end.

The point and interval prediction of the time to endpoint maturation has been extensively studied in the literature (Bagiella & Heitjan, 2001; T. T. Chen, 2016; Y. Lan & Heitjan, 2018; Machida et al., 2025; shuang Ying et al., 2017; G. S. Ying & Heitjan, 2008, 2013; G.-S. Ying et al., 2004). Heitjan et al. (Heitjan et al., 2015) provide a comprehensive review of existing methods, highlighting the importance of prediction intervals for time to endpoint maturation to quantify uncertainty around the study's closing date. Some approaches accommodate ongoing accrual at the time of prediction (V. V. Anisimov, 2011; L. Wang et al., 2022; X. Zhang & Long, 2012).

Predicting the additional number of events at interim time points is critical for decision-making, especially when new drugs are being developed at a fast pace and adaptive and complex trials designs are increasingly needed, e.g. platform trials. Nevertheless, most available methods in the biostatistical literature provide only point prediction under a few survival distributions. Fang and Su (Fang & Su, 2011) proposed a hybrid approach that combines nonparametric and parametric modeling to estimate the survival curve. Specifically, change points in the survival function are first detected using a data-driven algorithm developed by Goodman et al. (Goodman et al., 2011). The segment preceding the final change point is estimated nonparametrically, while the tail beyond it is modeled using a parametric exponential or Weibull distribution. This approach is implemented by Rufibach (Rufibach, 2025) in the *eventTrack* R package. A growing body of literature has also addressed the use of point prediction for the purpose of sample size re-estimation (Friede et al., 2019; Hade et al., 2010; Mori et al., 2024; Todd et al., 2012; Whitehead, 2001). Even though point predictions are easy to communicate they do not quantify uncertainty about reaching the planned information level and target number of events by the prespecified date. Prediction intervals address this limitation by explicitly reflecting uncertainty through their limits and width, making them more informative for interim trial monitoring. To the best of our knowledge, only two approaches address directly the issue of providing prediction interval for the additional number of events. Anisimov (V. V. Anisimov, 2011) derived closed-form prediction intervals for the number of future events in ongoing multicenter time-to-event trials, explicitly accounting for both newly recruited and at-risk patients under varied recruitment scenarios. The approach models center-level accrual via a Poisson–gamma process and event dynamics with continuous-time finite Markov chains under an exponential model. Anisimov et al. (V. Anisimov et al., 2021) extended the framework to incorporate a cure fraction, under both exponential and Weibull assumptions. However, these approaches construct prediction intervals using the so-called plug-in method (Meeker et al., 2017), i.e., they treat the model parameters as if they were known and simply replace them with their point estimates when computing the conditional distribution of the additional number of events. This has been shown to yield intervals whose coverage can be far from the nominal level (Tian et al., 2022). Motivated by a recently completed phase III trial in childhood acute lymphoblast leukemia (ALL), we propose here a general framework to construct prediction intervals for the additional number of events at interim analysis in fixed follow-up times clinical trials by adapting and extending a method originally developed in reliability engineering for predicting component failures (Tian et al., 2022). We extended the approach to the clinical setting by treating the patient (rather than a component cohort) as the unit of analysis, accommodating possible dependence between entry dates and loss to follow-up and leveraging patient-level covariates available for instance in case of at unblinded interim looks.

This paper is organized as follows: Section 2 introduces the notation, the prediction framework and briefly reviews the methods originally proposed by Tian et al. (Tian et al., 2022) for obtain prediction intervals; Section 3 outlines our proposed adaptation and extensions; Section 4, presents the results of a simulation study to evaluate the performance of the modified framework; Section 5 include an application to a phase III trial in childhood acute lymphoblast leukemia (ALL); Section 6 discusses the implications of our findings and highlights potential extensions.

## 2 Background

The framework proposed by Tian et al. (Tian et al., 2022) was developed in the context of reliability engineering. Given a sample of items inspected at a given time, the aim is to provide prediction intervals for the number of inspected items that will fail within a future time window, which constitutes a within-sample prediction problem. The authors consider two reliability settings: a *single-cohort scenario*, where a homogeneous set of units enters testing at the same time, and a *multiple-cohort scenario*, where homogeneous sets enter at different times.

For both scenarios, Tian et al. (Tian et al., 2022) propose three bootstrap-based approaches that extend the prediction-interval constructions reviewed in Appendix, Section 7.1 to within-sample prediction with censored survival data: the *direct bootstrap*, building on (Harris, 1989) (Shen et al., 2018), the *calibration bootstrap* following (Beran, 1990), and a *generalized pivotal-quantity* approach, which uses bootstrap to approximate the distribution of a generalized pivotal quantity for  $\vartheta$  in log-location-scale models, following (Hannig et al., 2006) (C. M. Wang et al., 2012).

In this paper, we adapt and extend the *direct bootstrap* method in the *multiple-chort* scenario. Tian et al. (Tian et al., 2022) show that the method has stronger empirical performance than the *calibration bootstrap*. Moreover, unlike the *generalized pivotal-quantity* bootstrap—whose construction is primarily well-defined under Type II censoring and only approximated under Type I censoring—the *direct bootstrap* can accommodate more general censoring mechanisms. We therefore focus on this approach and briefly describe it below.

### 2.1 Prediction Intervals Definition

Let  $\mathbf{D}$  denote the observed sample of  $n$  independent and identically distributed observations arising from a time-to-event process and, possibly, an additional censoring process, with joint density indexed by the parameter vector  $\vartheta$ . Here,  $\vartheta$  collects the parameters governing the time-to-event distribution and, when applicable, those of the censoring distribution. At a fixed time  $t_c$  we are interested in predict the value of a future discrete random variable  $Y$ , i.e. the predictand, here the additional number of events, which has conditional cumulative mass function (CMF)  $F_Y(y|\mathbf{D}; \pi)$ , depending on  $\pi = \varphi(\vartheta)$ . We introduce the notation  $\mathcal{D}$ ,  $L(\mathcal{D})$  and  $U(\mathcal{D})$  for the sample space of  $\mathbf{D}$ , the lower and upper prediction bounds for  $Y$  respectively. If  $L(\mathcal{D})$  and  $U(\mathcal{D})$  are determined so that

$$P(L(\mathcal{D}) \leq Y \leq U(\mathcal{D})) = 1 - \alpha, \quad (1)$$

then  $\text{PI}_{1-\alpha}(\mathcal{D}) = [L(\mathcal{D}), U(\mathcal{D})]$  is called a  $1 - \alpha$  level prediction interval for  $Y$  and  $\text{PI}_{1-\alpha}(\mathbf{D})$  denote its realization. We restrict our attention to two-sided prediction intervals, thus requiring that  $L(\mathcal{D})$  and  $U(\mathcal{D})$  be both finite. A prediction interval is exact if (1) is exactly equal to  $1 - \alpha$ , while it is asymptotically correct if  $\lim_{n \rightarrow \infty} P(L(\mathcal{D}) \leq Y \leq U(\mathcal{D})) \rightarrow 1 - \alpha$ , as is often the case for a discrete predictand.

Some comments on the relationship between  $Y$  and  $\mathbf{D}$  are in order. In new-sample prediction (also known as out-of-sample prediction), the predictand belongs to a future, independent sample under the assumed model, so  $Y$  is independent of  $\mathbf{D}$ . In within-sample prediction (also known as forecast), the predictand represents a random variable belonging to the same sample for which the prediction is made in the future (Meeker et al., 2017). In this case,  $Y$  and  $\mathbf{D}$  are not independent. This scenario is common in both reliability analysis and interim monitoring settings. In the within-sample case, all the methods proposed by Tian et al. (Tian et al., 2022) are supported by theoretical guarantees of asymptotic nominal coverage in contrast to the plug-in method that is valid only for a new-sample prediction contest. In the plug-in method (also known as naive or estimative), prediction intervals are recovered from  $F_Y(y|\mathbf{D}; \hat{\pi})$ , where  $\hat{\pi}$  is a consistent estimator of  $\pi$ .

### 2.2 The Direct-bootstrap, Multiple Chort Method (DB-MC)

At the prediction time  $t_c$ , there are  $g$  cohorts (groups) of items. Cohort  $j$  contains  $n_j$  items that were put on test at the common known entry time  $\tau_{aj}$ , with  $j = 1, \dots, g$ . Let  $T_{ij}$  denote the failure time of item  $i$  in cohort  $j$ , and assume

$$T_{ij} \stackrel{\text{iid}}{\sim} f_{\vartheta}(t), \quad i = 1, \dots, n_j, \quad j = 1, \dots, g, \quad (2)$$

where all items share the same (common) PDF  $f_{\vartheta}(t)$ . Define the event indicator at  $t_c$  for item  $i$  in cohort  $j$  as  $\tilde{\delta}_{ij} = \mathbb{I}(T_{ij} \leq \tau_j)$  where  $\tau_j = t_c - \tau_{aj}$ . The number of observed failures in cohort  $j$  is  $\delta_j = \sum_{i=1}^{n_j} \tilde{\delta}_{ij}$  and the number of right-censored items is  $\gamma_j = n_j - \delta_j$ . The data observed at  $t_c$  can be represented as a collection of single-cohort datasets,  $\mathbf{D} = \{D_1, \dots, D_g\}$ . For cohort  $j$ , we summarize the observed information as  $D_j = (\mathbf{T}_j, \delta_j, \gamma_j)$ , where  $\mathbf{T}_j$  is the vector of observed times possibly right-censored,  $\delta_j$  denotes the number of failures, and  $\gamma_j$  the number of units censored at  $t_c$ .

Let  $Y$  be the number of item failures to be predicted at a future time  $\tau_j + \Delta t$  on  $n = \sum_{j=1}^g n_j$  tested unit. We denote  $\zeta_j = \sum_{i=1}^{n_j} \mathbb{I}(\tau_j < T_{ij} \leq \tau_j + \Delta t)$ . Since  $\zeta_j \sim \text{Bin}(\pi_j, \gamma_j)$  are mutually independent and  $\pi_j = P(T_j \leq \tau_j + \Delta t | T_j > \tau_j)$ , then

$$Y = \sum_{j=1}^g \zeta_j \sim \text{PoiBin}(\boldsymbol{\pi}, \boldsymbol{\gamma}), \quad (3)$$

where  $\text{PoiBin}(\boldsymbol{\pi}, \boldsymbol{\gamma})$  denotes the probability mass function (PMF) of a Poisson-binomial distribution with probability vector  $\boldsymbol{\pi} = (\pi_1, \dots, \pi_g)$ , weight vector of the at risk units  $\boldsymbol{\gamma} = (\gamma_1, \dots, \gamma_g)$  (Hong, 2013) (Tang & Tang, 2022). We briefly review the PMF and the CMF of the Poisson-binomial distribution in the Appendix, Section 7.2.

Following (Harris, 1989), Tian et al. (Tian et al., 2022) proposed obtaining the  $1 - \alpha$  prediction interval for  $Y$  as the corresponding quantiles of the bootstrap estimator of the conditional CMF. Specifically, once  $\mathbf{D} = \{D_1, \dots, D_g\}$  is observed, estimate  $\hat{\boldsymbol{\theta}}$  for  $\boldsymbol{\theta}$  is found by maximizing the parametric likelihood

$$\mathcal{L}(\boldsymbol{\theta}) \propto \prod_{j=1}^g \prod_{i=1}^{n_j} f_{\boldsymbol{\theta}}(t)^{\tilde{\delta}_i} \left[1 - F_{\boldsymbol{\theta}}(t)\right]^{1-\tilde{\delta}_i}, \quad (4)$$

where  $F_{\boldsymbol{\theta}}(t)$  is the CDF of  $T_{ij}$ . Thus, one generates  $B$  bootstrap replications of the *multiple-cohort* data from  $f_{\hat{\boldsymbol{\theta}}}(t)$  and, for each replication  $b = 1, \dots, B$ , computes the vector  $\hat{\boldsymbol{\pi}}_b^*$  of cohort-specific conditional event-probability at a future prediction horizon  $\Delta t$ . For each bootstrap sample, one then evaluates the CMF of  $Y$ , denotes as  $F_Y(y | \hat{\boldsymbol{\pi}}_b^*)$ . Averaging these over  $b$  yields the direct-bootstrap estimator of the conditional CMF is (Tian et al., 2022)

$$\hat{F}_Y^*(y | \mathbf{D}) = \frac{1}{B} \sum_{b=1}^B F_Y(y | \mathbf{D}_b^*; \hat{\boldsymbol{\pi}}_b^*). \quad (5)$$

Thus, a  $1 - \alpha$  equal-tails prediction interval is given by

$$\text{PI}_{1-\alpha}(\mathbf{D}) = \{y : y_{\alpha/2}^* \leq y \leq y_{1-\alpha/2}^*\}, \quad (6)$$

where  $\mathcal{D} = \mathbf{D}$  denotes the observed sample and  $y^*$  and  $y_{1-\alpha/2}^*$  are the  $\alpha/2$  and  $1 - \alpha/2$  quantiles of the bootstrap estimator of the CMF of  $Y$  (See Appendix, Section 7.1 for details). In terms of coverage, the method is supported by theoretical guarantees of asymptotic nominal coverage. (Theorem 1, 2, 3 in Tian et al., 2022).

### 3 Extension to the Interim Monitoring Setting

The DB–MC method in Section 2.2 closely matches the clinical trial setting, as it naturally accommodates staggered entry and censoring at the interim cutoff by treating each patient enrolled up to the interim date as a cohort of size one. This combination of patient-specific entry times and a common prespecified cutoff that sets the admissible follow-up is often referred to as *generalized type I censoring* (Klein & Moeschberger, 2003). In interim monitoring, however, additional right censoring mechanisms may operate beyond generalized type I censoring, most notably random censoring due to loss to follow-up. A further key distinction from the original DB–MC setting is that phase III trials typically exhibit patient-level heterogeneity—driven by randomized treatment allocation and other covariates—which can be leveraged to improve prediction, especially under unblinded monitoring for early efficacy or futility. These extensions are the focus of our work. We consider phase III trials with closed accrual at the prediction time, consistent with our motivating example and Tian et al. (Tian et al., 2022).

#### 3.1 Methods

At the interim time  $t_c$ , accrual is closed and  $n$  patients are available, each with a specific entry time  $\mathcal{T}_{aj}$ ,  $j = 1, \dots, n$ . Let  $T_j$  denote the time to event and  $L_j$  the time to loss to follow-up, both measured from study entry. Define the individual censoring time at the interim as  $\mathcal{T}_j = t_c - \mathcal{T}_{aj}$ . Let  $C_j = \min(L_j, \mathcal{T}_j)$ ,  $T_j^{\text{obs}} = \min(T_j, C_j)$ , and define the event-type indicators  $\delta_j = \mathbb{I}(T_j \leq C_j)$ ,  $\varepsilon_j = \mathbb{I}(L_j \leq \min(T_j, \mathcal{T}_j))$ ,  $\gamma_j = \mathbb{I}(\mathcal{T}_j \leq \min(T_j, L_j))$ . Finally, let  $\mathbf{z}_j$  denote the vector of patient-level covariates. Here we focus on baseline characteristics. We impose the following assumptions

on  $(T_j, L_j, \mathcal{T}_j)$ :

- (A1)  $T_j \stackrel{\text{iid}}{\sim} f_{\boldsymbol{\theta}}(t \mid \mathbf{z}_j)$ .
- (A2)  $(L_j, \mathcal{T}_j) \stackrel{\text{iid}}{\sim} g_{\boldsymbol{\psi}, \boldsymbol{\phi}}(l, \tau)$ .
- (A3)  $T_j \perp (L_j, \mathcal{T}_j) \mid \mathbf{z}_j$ .
- (A4)  $\boldsymbol{\vartheta} = (\boldsymbol{\theta}, \boldsymbol{\psi}, \boldsymbol{\phi}) \in \Theta \times \Psi \times \Phi$ .

Note that, since patients enter the study at random calendar times, the distribution of  $\mathcal{T}_j$  is induced by the distribution of entry times  $\mathcal{T}_{aj}$ , shifted by  $t_c$  (i.e.,  $\mathcal{T}_j = t_c - \mathcal{T}_{aj}$ ); see Jiang et al., 2021. Thus, we assume an independent right-censoring mechanism, identical across treatment groups and covariate levels and that the PDFs of  $T_j$ ,  $L_j$  and  $\mathcal{T}_j$  do not share any parameters. In contrast, interim censoring and loss to follow-up are not required to be independent processes, that is, we do not require that  $g_{\boldsymbol{\psi}, \boldsymbol{\phi}}(l, \tau) = \tilde{g}_{\boldsymbol{\psi}}(l) r_{\boldsymbol{\phi}}(\tau)$ , where  $\tilde{g}_{\boldsymbol{\psi}}(l)$  and  $r_{\boldsymbol{\phi}}(\tau)$  are the marginal distribution of  $L_j$  and  $\mathcal{T}_j$  respectively. This implies that we do not account for any potential dependence between the loss-to-follow-up times and the entry times, e.g., patients enrolled near the end of accrual may therefore be less likely to be loss to follow-up (Jiang et al., 2021).

Let  $Y$  be the number of events to be predicted at a future time  $\tau_j + \Delta t$  where  $\tau_j = t_c - \tau_{aj}$  denotes a realization of  $\mathcal{T}_j$ . Furthermore, let  $\zeta_j$  be the indicator function for  $T_j \leq \min(\tau_j + \Delta t, L_j)$ . The probability that a patient will experience the event by the future time  $\tau_j + \Delta t$ , given that neither he/she has not yet experienced the event at the time of the interim  $t_c$  neither was loss to follow-up is  $\pi_j = \Pr(T_j \leq \min(\tau_j + \Delta t, L_j) \mid \gamma_j = 1, \mathbf{z}_j)$ . Under assumptions (7),  $\pi_j$  can be expressed as

$$\pi_j = \frac{[F_{\boldsymbol{\theta}}(\tau_j + \Delta t \mid \mathbf{z}_j) - F_{\boldsymbol{\theta}}(\tau_j \mid \mathbf{z}_j)] - \int_{\tau_j}^{\tau_j + \Delta t} \tilde{G}_{\boldsymbol{\psi}}(u) f_{\boldsymbol{\theta}}(u \mid \mathbf{z}_j) du}{[1 - F_{\boldsymbol{\theta}}(\tau_j \mid \mathbf{z}_j)] [1 - \tilde{G}_{\boldsymbol{\psi}}(\tau_j)]}, \quad (8)$$

where  $F_{\boldsymbol{\theta}}$  and  $\tilde{G}_{\boldsymbol{\psi}}$  are the CDFs of the event time and loss to follow-up time respectively. Proof of (8) and special cases are given in Appendix, Section 7.3. Since  $\zeta_j \sim \text{Ber}(\pi_j) = \text{Bin}(\pi_j, 1)$  and are assumed mutually independent, the number of events to be predicted at a future time  $\tau_j + \Delta t$  has still a Poisson-binomial distribution, that is

$$Y = \sum_{j: \gamma_j=1} \zeta_j \sim \text{PoiBin}(\boldsymbol{\pi}), \quad (9)$$

where  $\boldsymbol{\pi}$  is the vector of individual conditional probabilities obtained for only the interim censored patients as in (8). Prediction bounds are then obtained as in (6) after having recovered the bootstrap estimator of the conditional CMF. Once the interim data  $\mathbf{D} = (T_j^{\text{obs}}, \delta_j, \varepsilon_j, \gamma_j, \mathbf{z}_j)_{j=1}^n$  is observed, estimates for  $\boldsymbol{\theta}$  and  $\boldsymbol{\psi}$  are found by maximizing the following parametric likelihoods

$$\begin{aligned} \mathcal{L}(\boldsymbol{\theta}) &\propto \prod_{j=1}^n f_{\boldsymbol{\theta}}(t \mid \mathbf{z}_j)^{\delta_j} \left[1 - F_{\boldsymbol{\theta}}(t \mid \mathbf{z}_j)\right]^{1-\delta_j}, \\ \mathcal{L}(\boldsymbol{\psi}) &\propto \prod_{j=1}^n \tilde{g}_{\boldsymbol{\psi}}(l)^{\varepsilon_j} \left[1 - \tilde{G}_{\boldsymbol{\psi}}(l)\right]^{1-\varepsilon_j}, \end{aligned} \quad (10)$$

Maximizing the likelihoods in (10) is justified under assumptions (7) and yields the maximum likelihood estimator for  $\boldsymbol{\theta}$  and  $\boldsymbol{\psi}$ . This justification is given in the Appendix, Section 7.4.

### 3.2 Proposed Sampling Scheme

The original DB–MC method requires generating many replicates of the multiple-cohort dataset and, for each replicate, computing the vector of conditional probabilities  $\boldsymbol{\pi}$  at a future prediction horizon  $\Delta t$ . Translating this step to interim monitoring—where each patient can be viewed as a cohort of size one—requires additional care. We propose a parametric bootstrap sampling scheme to obtain the bootstrap estimator if the conditional CMF of  $Y$ . The proposed scheme is exposed in the Appendix, Section 7.5.

Some remarks are worth noting regarding the nature of the inference considered in this particular contest. The proposed sampling scheme conditions on the event and censoring indicators, i.e, they are kept fixed across bootstrap replicates. If censoring indicators were different as in classic survival bootstrap (Akritas, 1986; Bilker & Wang, 1997; Efron, 1981; Gross & Lai, 1996; Hjort, 1985), the risk set would vary across replicates and the Monte Carlo average in (5) would mix conditional CMFs with different supports. This would target an *unconditional* CMF, whereas in a within-sample prediction problem it is required the CMF of  $Y$  *conditional* on the observed risk set that defines its support. Conditioning on the indicators also brings information on the observed times. Moreover, each  $\pi_j$  is conditional on  $\tau_j$ . Hence, the bootstrap must preserve this conditioning in order to recover the sampling distribution of  $\pi$  at a future prediction horizon  $\Delta t$ . Prior observing the interim data  $\mathbf{D}$ ,  $(T_j^{\text{obs}}, \delta_j, \varepsilon_j, \gamma_j)_{j=1}^n$  are random variables with PDF  $\Pr_{\boldsymbol{\theta}}(T_j^{\text{obs}}, \delta_j, \varepsilon_j, \gamma_j \mid \mathbf{z}_j)$ . Once observing the indicators values and fixing the entry dates, we have

$$\begin{aligned} \Pr(T_j^{\text{obs}} = t \mid \delta_j = 1, \mathbf{z}_j) &= \frac{f_{\boldsymbol{\theta}}(t \mid \mathbf{z}_j)}{F_{\boldsymbol{\theta}}(\tau_j \mid \mathbf{z}_j)}, \\ \Pr(T_j^{\text{obs}} = t \mid \varepsilon_j = 1) &= \frac{\tilde{g}_{\boldsymbol{\psi}}(t)}{\tilde{G}_{\boldsymbol{\psi}}(\tau_j)}. \end{aligned} \quad (11)$$

It follows that event times and loss-to-follow-up times are sampled from their respective truncated PDFs in (11), whereas interim censoring times are kept fixed at their realized values, thus ignoring how they are distributed. Sampling event times and loss-to-follow-up times from (11) can be carried out straightforwardly via inverse-transform. This approach is flexible and accommodates a wide range of lifetime distributions, requiring only evaluation of the corresponding truncated PDF and its inverse (Bender et al., 2005) (Crowther & Lambert, 2013). See Appendix, Section 7.5 for further details. In each bootstrap replicate, we obtain  $\hat{\boldsymbol{\theta}}$  and  $\hat{\boldsymbol{\psi}}$  by maximizing the likelihood in (10) under the same assumptions, and then compute  $\pi_j$  at a future prediction horizon  $\Delta t$  accordingly.

## 4 Simulation Study

We conducted two comprehensive simulation studies to globally assess the operating characteristics of the proposed method under various conditions of interest in the interim analysis contest. Our simulations not only assess the impact of the proposed extensions, but also investigate the behavior of the original DB-MC method.

### 4.1 Data generating process

We considered two simulation studies with different data generating processes and experimental conditions, namely  $\mathcal{S}_1$  and  $\mathcal{S}_2$ . In  $\mathcal{S}_1$  data were generated from Weibull proportional hazards model with uniform entry dates over three years of recruitment period. In addition, we introduce an exponential loss-to-follow-up mechanism that is correlated with entry time, so that patients enrolled earlier are more likely to be loss to follow-up than those enrolled later. To induce this dependence while keeping the entry-time and loss-to-follow-up marginals PDFs parameterized separately, we use NORTA sampling (NORmal To Anything) (Carlo & Nelson, 1997) and calibrate the target correlation via a bisection procedure (Austin, 2023) with tolerance 0.001 and a maximum of 100 iterations with sample size 20000. The Weibull shape parameter was fixed at 0.6 (decreasing hazard). The baseline scale parameter was varied so that the proportion of interim censored observations matched the target censoring proportion under a specific value of the hazard ratio (see next Section), using also a bisection procedure (Austin, 2023) with starting value 0, tolerance 0.001, and a maximum of 300 iterations. We considered treatment as covariate, assuming a 1:1 randomization ratio generated from a Bernoulli distribution with parameter 0.5. The Poisson–binomial distribution was approximated in each bootstrap sample by a Poisson distribution, as Hong (Hong, 2013) showed this approximation to be highly accurate for a moderately large number of Bernoulli trials (e.g.  $>200$ ) while being computationally more efficient than exact methods.

In  $\mathcal{S}_2$ , the data-generating process is similar  $\mathcal{S}_1$  but we imposed only administrative censoring at the interim cutoff. Full details of the generating mechanisms and the resulting parameter values are reported in the Appendix, Section 7.6.

### 4.2 Factors in the simulations

In  $\mathcal{S}_1$ , the performance of the proposed method is evaluated over 72 scenarios defined by a combination of the following factors: the correlation between the loss to follow-up distribution and the entry dates  $\rho = \{0.1, 0.5\}$ , the follow-up maturity at the time of prediction,  $t_c = \{1, 2, 4\}$ , expressed as the time from accrual end to the interim look; the ratio between the baseline Weibull scale and the loss to follow-up rate,  $k = \{0.1, 0.2, 0.3\}$ ; the strength of the treatment

effect, expressed by the hazard ratio,  $HR = \{0.2, 0.8\}$ ; and the future prediction horizon,  $\Delta t = \{1, 4\}$ . The proportion of interim censored observations is fixed at 0.5. Here, we evaluate prediction intervals under correct model specification.

In  $\mathcal{S}_2$ , the methodology is evaluated over 24 scenarios defined by a combination of the following factors: the proportion of interim censored observations,  $0.2 = \{0.2, 0.8\}$  and  $t_c$ ,  $HR$ ,  $\Delta t$  using the same values defined in  $\mathcal{S}_1$ . We evaluated prediction intervals obtained from the Weibull model, Royston–Parmar models with 1, 2, and 3 knots placed at the 25th, 50th, and 75th percentiles of the uncensored event times and the Generalized Gamma model (Stacy, 1962), which encompasses Weibull and log-normal as special cases (Prentice, 1975) (Cox et al., 2007). Following Mori et al. (Mori et al., 2024), we decided to include Royston–Parmar models (Royston & Parmar, 2002) as a flexible extension of standard parametric regression models. These models generalize the linear relationship between a transformed survival function, i.e. a link function  $g(S(t))$  and log time  $y = \log(t)$  on a chosen covariates effect scale (e.g. proportional hazard scale) by modeling this relationship with restricted cubic splines. In this sense, they extend the Weibull proportional hazards model, the log-logistic proportional odds model, and the log-normal linear probit model. Despite their added flexibility, Royston–Parmar models preserve an explicit baseline specification, allowing extrapolation beyond the last observed event. Flexibility is controlled by the number of internal knots placed between boundary knots (Royston & Parmar, 2002).

For each combination of factors, the metrics were computed and averaged on  $N = 1000$  Monte Carlo samples with sample size  $n = 1000$ . For each simulated dataset, 100 bootstrap resamples were used to construct the prediction intervals. Although 100 bootstrap replicates is relatively modest, this choice was necessary to keep the overall computational burden manageable across all scenarios.

### 4.3 Performance metrics

The prediction intervals obtained within the DB-MC framework enjoy the classical frequentist interpretation: they correspond to the long-run proportion of times that  $Y$  falls in a random region  $\text{PI}_{1-\alpha}(\mathcal{D})$ , i.e. the prediction interval, under repeated sampling from the same data-generating mechanism (Barndorff-Nielsen & Cox, 1996; Lawless & Fredette, 2005). Coverage probability (CP) is a useful performance metric to evaluate an interval estimator. Since  $Y$  is also random, there are two natural notions of CP associated with a prediction interval procedure (Beran, 1990; Meeker & Escobar, 1998). First, for the observed data  $\mathbf{D}$  there is the coverage probability of the realized prediction interval, i.e., the conditional coverage probability (CCP)

$$\text{CCP} = P(Y \in \text{PI}_{1-\alpha}(\mathbf{D}) \mid \varphi(\boldsymbol{\vartheta})). \quad (12)$$

After observing  $\mathbf{D}$  and obtaining  $\text{PI}_{1-\alpha}(\mathbf{D})$ , we can use an estimate  $\varphi(\hat{\boldsymbol{\vartheta}})$  of the unknown parameters to estimate the CCP. Although this retains a meaningful interpretation – in contrast with confidence intervals, for which the realized interval has coverage probability either 0 or 1 – the CCP refers to one specific realization of  $\mathbf{D}$  and it is not informative of the average behavior of the prediction interval procedure. Moreover, CCP itself depends on  $\mathbf{D}$  and is therefore a random quantity. This motivates the unconditional coverage probability (UCP), defined as

$$\begin{aligned} \text{UCP} &= \mathbb{E}_{\mathcal{D}}[\text{CCP} \mid \varphi(\boldsymbol{\vartheta})] \\ &= \mathbb{E}_{\mathcal{D}}[\Pr\{Y \in \text{PI}_{1-\alpha}(\mathbf{D}) \mid \varphi(\boldsymbol{\vartheta})\}] \\ &= P(Y \in \text{PI}_{1-\alpha}(\mathcal{D}) \mid \varphi(\boldsymbol{\vartheta})). \end{aligned} \quad (13)$$

When a closed-form expression for (13) is not available, UCP can be approximated by Monte Carlo simulation (Mee & Kushary, 1994) (Meeker et al., 2017)) as

$$\text{UCP} \approx \frac{1}{N} \sum_{k=1}^N P(Y \in \text{PI}_{1-\alpha}(\mathbf{D}_k^*)), \quad (14)$$

where  $\mathbf{D}_1^*, \dots, \mathbf{D}_N^*$  are simulated data from a given model. In our simulation studies,  $\boldsymbol{\vartheta} = (\boldsymbol{\theta}, \boldsymbol{\psi}, \boldsymbol{\phi})$  and  $\varphi(\boldsymbol{\vartheta}) = \boldsymbol{\pi}$ . The UCP of the prediction intervals is estimated under the factors described in Section 4.2 using the following steps:

1. Generate  $N$  independent samples  $\mathbf{D}_k^*$  under the data-generating processes detailed in Section 4.1.
2. For each simulated sample, obtain the prediction interval  $\text{PI}_{1-\alpha}(\mathbf{D}_k^*)$  by applying the proposed parametric bootstrap scheme to obtain the conditional CMF of  $Y$  and by taking the corresponding  $\alpha/2$  and  $1 - \alpha/2$  quantiles. For  $\mathcal{S}_2$  we obtain the quantiles under different parametric models (See Section 4.1).
3. For each  $\mathbf{D}_k^*$ , we evaluate the CCP using the conditional distribution of  $Y$  evaluated at the true  $\boldsymbol{\pi}$ , i.e. the  $\boldsymbol{\pi}$  evaluated on the simulated dataset  $\mathbf{D}_k^*$  at the design value of  $\boldsymbol{\vartheta}$ .

#### 4. Average these evaluations as in (14).

The closer the estimated prediction bounds are to the  $\alpha/2$  and  $(1 - \alpha/2)$  quantiles of the conditional distribution of  $Y$  evaluated at the true  $\pi$  in each sample, the better the resulting coverage. For this reason, we additionally assess the relative bias of the estimated lower and upper prediction bounds, as well as the ratio between the width of the estimated interval and that of the true interval for the simulated dataset. These measures are respectively defined as

$$\begin{aligned} & \frac{y_\alpha(\mathbf{D}_k^*) - y_\alpha(\mathbf{D}_k^*, \pi)}{y_\alpha(\mathbf{D}_k^*, \pi)}, \\ & \frac{\text{PI}_{1-\alpha}(\mathbf{D}_k^*)}{\text{PI}_{1-\alpha}(\mathbf{D}_k^*, \pi)}. \end{aligned} \quad (15)$$

where  $y_\alpha(\mathbf{D}_k^*, \pi)$  and  $\text{PI}_{1-\alpha}(\mathbf{D}_k^*, \pi)$  are the  $\alpha$  quantile and the prediction interval obtained on the simulated dataset  $\mathbf{D}_k^*$  at the true value of  $\pi$ .

##### 4.3.1 Software

All simulations were performed in R 4.5.1 (R Core Team, 2025) and analyzed with the `rsimsum` package (Gasparini & White, 2024). Simulations from an (uncensored) Weibull regression model under a proportional hazards specification were generated using the `simsurv` package (Brilleman et al., 2020). Weibull models were fitted with the `survival` package (Therneau, 2020), whereas Generalized Gamma and Royston–Parmar models under proportional hazards were fitted with `flexsurv` (Jackson, 2024). Random variates from parametric survival models were obtained via the quantile functions implemented in `flexsurv`. Numerical integration was performed using the R function `integrate()`, which perform adaptive quadrature (R Core Team, 2025).

For the case study, nonparametric and semiparametric survival analyses were conducted using `survival` and `muhaz` (Hess & Gentleman, 2021). Weibull, log-normal, and log-logistic regression models were fitted with `survival`, while Generalized Gamma and Royston–Parmar models were fitted with `flexsurv`. Evaluation of the Poisson–Binomial distribution was carried out using the `poibin` package (Hong & R Core Team, 2024).

## 4.4 Results

In  $\mathcal{S}_1$ , overall coverage is close to the nominal level and it varies mainly with the prediction horizon  $\Delta t$  and follow-up maturity  $t_c$  (Figure 1). Longer horizons are associated with lower coverage, whereas more mature follow-up yields a modest improvement. Loss to follow-up also slightly reduces coverage, with a stronger impact for longer-term predictions. This pattern reflects a trade-off in information: higher loss to follow-up improves estimation of the censoring process but reduces information for estimating the event-time distribution.

Prediction intervals widen as  $\Delta t$  increases and  $t_c$  decreases, particularly when loss to follow-up is modest. However, wider intervals do not necessarily translate into higher coverage. Worsening occur mainly when both interval bounds shift in the same direction, producing intervals that are systematically biased upward (i.e., overestimating future event counts). Note that interval coverage here also reflects which portion of the support of the conditional predictive distribution is captured by the interval.

In  $\mathcal{S}_2$  under correct model specification, the prediction intervals maintained coverage close to the nominal level across almost all scenario combinations (Figure 2). Coverage deteriorated slightly only when follow-up maturity was low, the treatment effect was modest - hazard ratio equal to 0.8 - and predictions were made far beyond the interim time, with a maximal loss of about 5 percentage points.

Over-parameterised survival models were generally not inferior in terms of coverage compared with their nested counterparts, but this was achieved at the cost of wider intervals and systematically downward-biased bounds particularly in settings with substantial interim censoring. In contrast, the upper bounds of the predictive intervals behaved very similarly across models. Notably, for over-parameterised models the coverage deteriorated in scenarios with low follow-up maturity, especially when administrative censoring was limited, the hazard ratio was modest, and predictions were made far into the future. This loss of coverage was driven by a systematic underestimation of both lower and upper predictive limits, so that the resulting intervals tended to concentrate on the support of the conditional predictive distribution with relatively low true probability.

These patterns were particularly evident for the Royston–Parmar models (Figure 6, Appendix): increasing the number of spline knots, and hence model complexity, did not systematically improve performance. As follow-up maturity increased, coverage improved, but at the expense of wider intervals compared with the Generalized Gamma model.

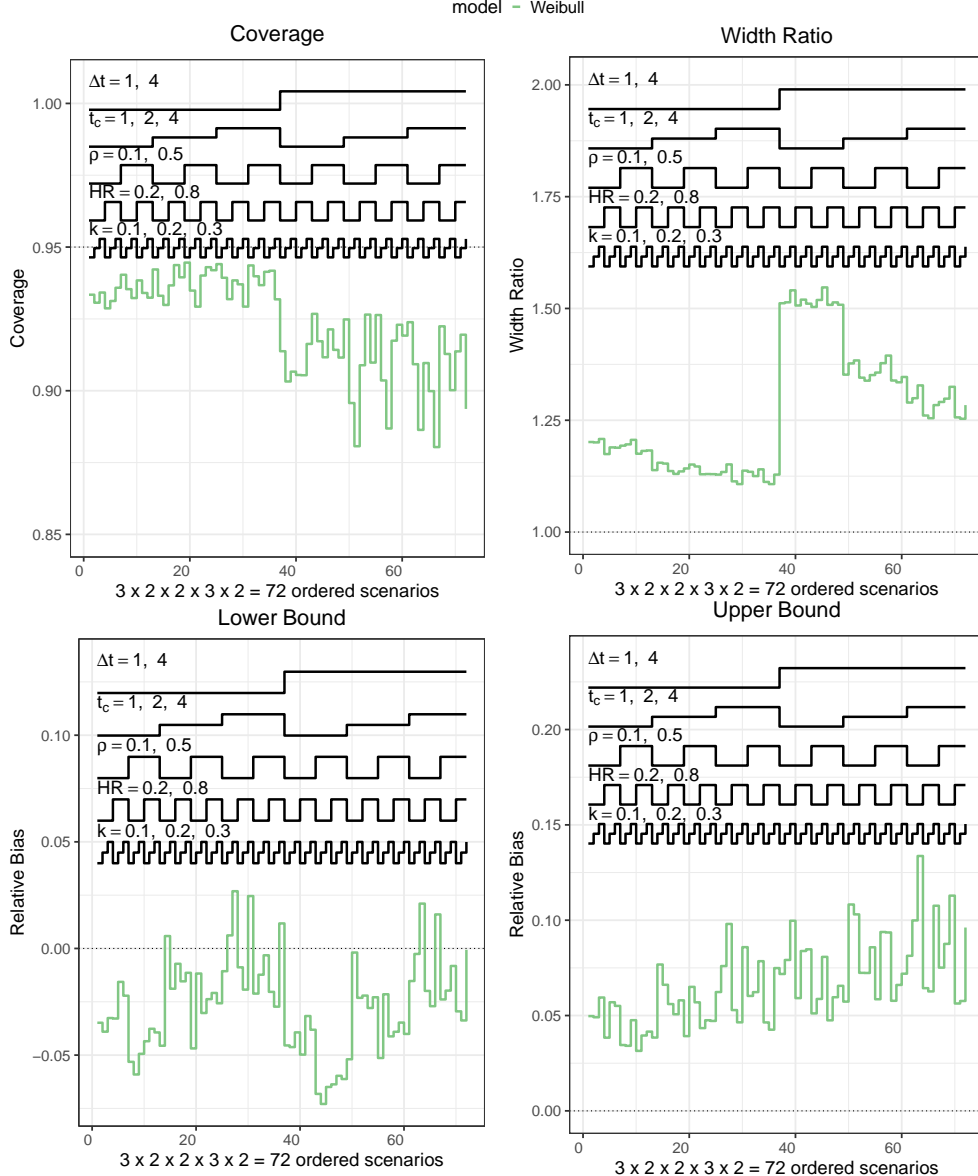


Figure 1: Study  $\mathcal{S}_1$ . Performance metrics of the 95% two-sided prediction intervals under different factors.  $\Delta t$  denotes the prediction horizon,  $t_c$  the time of interim from accrual end,  $\rho$  the correlation between loss to follow-up times and entry dates,  $HR$  is the hazard ratio and  $k$  the ratio between the baseline scale parameter and the loss to follow-up rate.

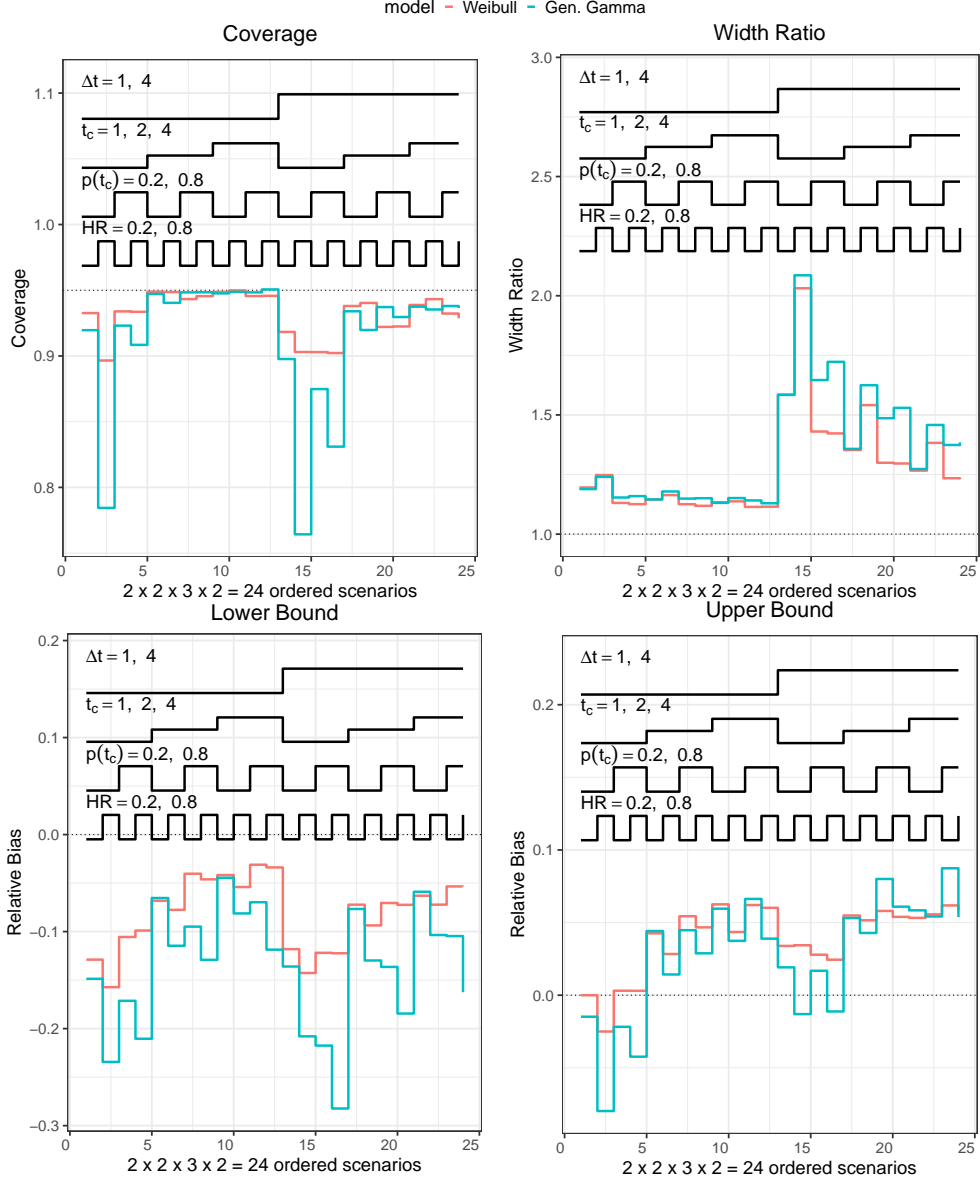


Figure 2: Study  $\mathcal{S}_2$ . Performance metrics of the 95% two-sided prediction intervals under different models and administrative censoring only at  $t_c$ .  $\Delta t$  denotes the prediction horizon,  $p(t_c)$  denotes the proportion of interim censored patients,  $t_c$  the time of interim from accrual end,  $HR$  is the hazard ratio and  $k$  the ratio between the baseline event rate and the loss to follow-up rate.

## 5 Case study in Pediatric ALL

To illustrate the proposed method, we considered data from a multicenter phase III trial on pediatric ALL published by Conter et al. (Conter et al., 2024). The AIEOP-BFM ALL 2009 protocol was an international, open-label, randomized phase III study conducted across seven countries and coordinated by the AIEOP-BFM consortium. The trial evaluated whether intensifying asparaginase exposure during early consolidation could reduce minimal residual disease (MRD) and improve outcomes in children and adolescents with high-risk ALL. In the experimental arm, patients received four additional weekly doses of pegylated L-asparaginase during Consolidation IB on top of standard chemotherapy, while the control arm followed the same regimen without PEG-ASNase. Between June 2010 and February 2017, 6136 children (aged 1–17 years) with Philadelphia-negative ALL were enrolled; 1097 met high-risk criteria at the end of induction and 809 were randomized, 404 experimental, 405 control. The primary endpoint was the proportion of

patients with PCR-MRD  $\geq 5 \times 10^{-4}$  at the end of consolidation. Secondary endpoints included event-free survival (EFS), overall survival (OS), cumulative incidence of relapse, and toxicity.

For the application of our method, two-sided prediction intervals at the 0.95 confidence level were obtained for the the number of additional EFS events from June 1, 2017 (accrual closure) and updated every six months until June 1, 2021, when the final analysis was scheduled. The full dataset was used to evaluate if the observed events are included by the prediction intervals. EFS is defined as the time from random assignment to the date of the first event (resistance to treatment, relapse, death, or second malignant neoplasm, whichever occurred first) or to the last follow-up. Since no loss to follow-up occurred at the time of the final analysis, all patients who had not experienced an EFS event by June 1, 2017 were considered administratively censored at that date. The presence of interim censoring only leads to a simplified formulation of (8) and the sampling scheme, as detailed in the Appendix, Section 7.3. On June 1 2017, 164 events had occurred among 809 enrolled patients. By the final analysis, 62 further events had been observed, for a total of 226 events over the entire trial.

We obtained prediction intervals under various regression models with treatment assignment as the only covariate. The baseline time-to-event distribution was specified as Weibull, Log-logistic, Log-normal, their Royston–Parmar counterparts — proportional hazards (PH), proportional odds (PO), and linear probit (LP) with 1, 2, or 3 internal knots placed at the 25th, 50th, and 75th percentiles of the uncensored event times — and the Generalized Gamma distribution. Model fit at interim was assessed both graphically and with information criteria. For a fitted model with log-likelihood  $\ell = \ell(\hat{\theta})$ ,  $q$  parameters and sample size  $n$ , we computed  $AIC = -2\ell + 2q$  and  $BIC = -2\ell + q \log n$ , where  $n$  denotes the number of uncensored observations. We used 5000 bootstrap samples to construct the prediction intervals and Poisson approximation was used to obtain the CMF of the Poisson-Binomial distribution in each sample.

Figure 3 shows the relationship between different transformations of the survival function and natural logarithm of time: straight parallel lines suggest correct specification of both baseline survival and covariates effect scale. These plots showed that there is no linear relationships between the transformed survival and the logarithm of time, suggesting that Royston–Parmar models may be adequate. In addition, PH assumptions are untenable. The smoothed hazard plot (Figure 7.9, Appendix) indicates decreasing hazards converging later in the follow-up.

Prediction intervals for the survival function obtained from simple parametric regression models (Weibull, log-logistic, and log-normal) were broadly similar across the prediction window and were consistently shifted upwards relative to the flexible counterparts (Figure 4). Within the Royston–Parmar models, different link functions (PH, PO, LP) produced comparable intervals and displayed a coherent pattern as the number of internal knots increased: specifications with 2–3 knots yielded wider and more downward-shifting prediction intervals as the prediction horizon lengthened, compared with the 1-knot models.

Model-fit comparisons based on information criteria (Table 1) highlight the trade-off between parsimony and goodness of fit. Although the maximized log-likelihoods were very similar across models, BIC tended to favor more parsimonious specifications, whereas AIC mainly separated simple parametric models from their more flexible counterparts. For instance, the log-normal model had the third-lowest BIC but one of the third-highest AIC values.

Model discrimination should also consider extrapolative performance. Inspection of the fitted hazard functions (Figures 9 to Figures 15, Appendix) showed that models imply different hazards, yet these differences matter for survival extrapolation primarily through the cumulative hazard function (Figures 16 to Figures 18, Appendix). Moreover, despite distinct baseline hazard shapes and different covariates effect scales, Weibull, log-logistic, and log-normal models have broadly similar standardized distributions within the log-location-scale family i.e., Gumbell, Logistic, Normal. Thus, they are expected to exhibit similar extrapolative performance despite having different fit. Analogous considerations apply to Royston–Parmar specifications.

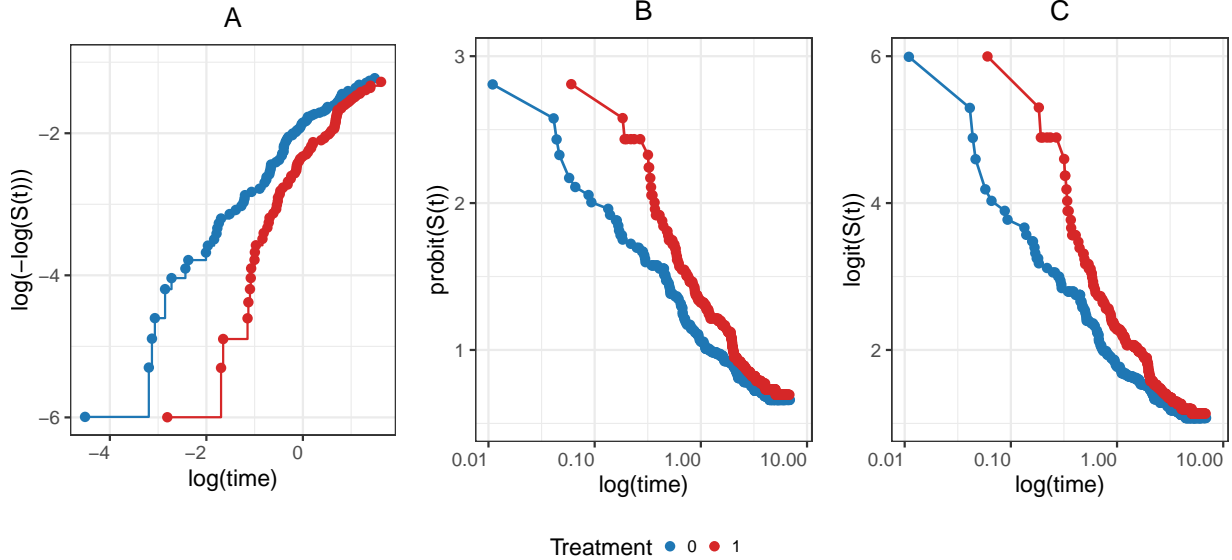


Figure 3: Different survival function transformations vs. log-time by treatment arm, 1 = Active treatment, 0 = standard of care. Panel A shows the log cumulative hazard of EFS  $\log(-\log(S(t)))$ ; Panel B shows the cumulative probit of EFS  $-\Phi^{-1}(S(t))$ , where  $\Phi^{-1}$  is CDF of the standard normal distribution; Panel C shows the cumulative logit of EFS  $\log(1 - S(t)/S(t))$ .

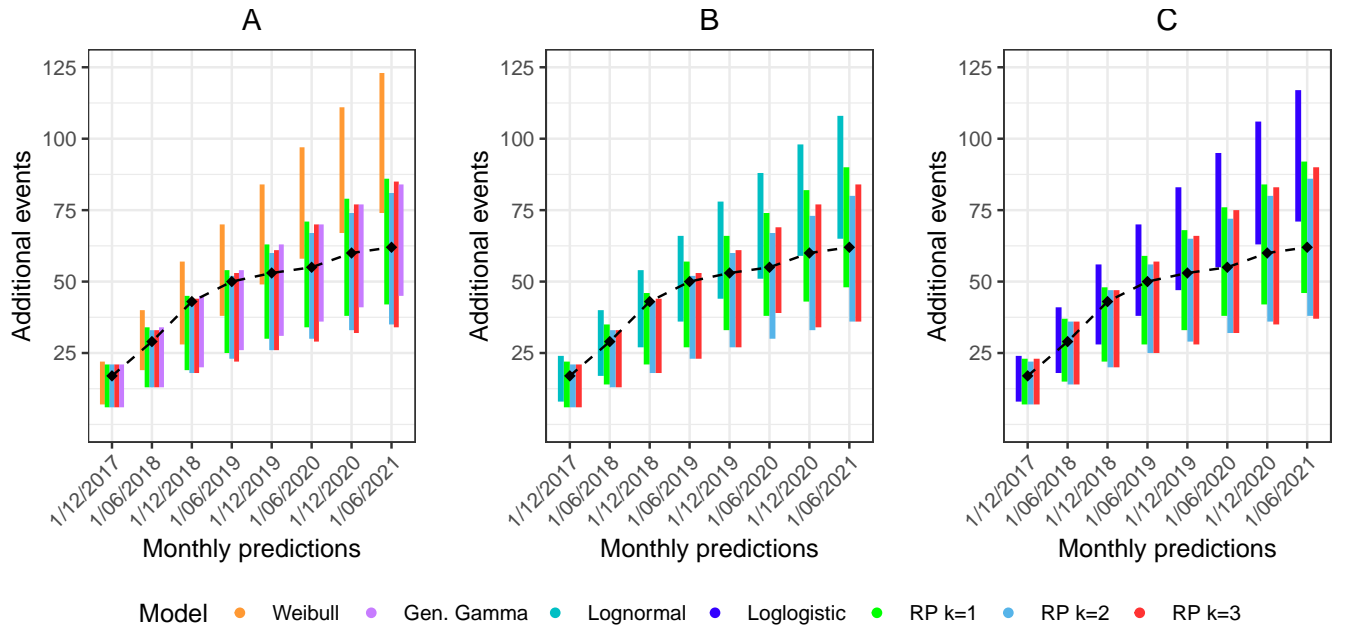


Figure 4: Two-sided 95% prediction intervals for the additional number of EFS events from June 1<sup>st</sup> 2017 to June 1<sup>st</sup> 2021. Black diamonds indicate the observed counts. Panel A shows intervals under the Weibull model and its flexible specifications; Panel B shows under the log-normal model and its flexible specifications; Panel C shows under the log-logistic model and its flexible specifications. RP = Royston–Parmar;  $k$  denotes the number of knots.

Table 1: Models fit measures

Model	<i>q</i>	<i>logLik</i>	<i>AIC</i>	<i>BIC</i>
Generalized Gamma	4	-562.9134	1133.827	1152.585
RP – PO(1)	4	-564.2135	1136.427	1155.185
Log-normal	3	-567.7988	1141.598	1155.666
RP – PH(1)	4	-564.6479	1137.296	1156.054
RP – LP(1)	4	-564.6479	1137.296	1156.054
RP – PH(2)	5	-562.1776	1134.355	1157.803
RP – LP(2)	5	-562.1776	1134.355	1157.803
RP – PO(2)	5	-563.1182	1136.236	1159.684
RP – PH(3)	6	-561.4914	1134.983	1163.120
RP – LP(3)	6	-561.4914	1134.983	1163.120
RP – PO(3)	6	-562.4590	1136.918	1165.056
Log-logistic	3	-573.9548	1153.910	1167.978
Weibull	3	-576.7842	1159.568	1173.637

*Note:* Models are ordered by increasing BIC. *q* denotes the number of parameters. RP = Royston–Parmar model, PH(*k*) = Proportional Hazards, PO(*k*) = Proportional Odds, LP(*k*) = Linear Probit, where *k* denotes the number of knots.

## 6 Discussion and Conclusions

In this work, we propose a general framework to predict the additional number of events during interim monitoring of clinical trials with time-to-event endpoints, together with corresponding prediction intervals. The framework accommodates patient-level covariates, loss to follow-up, and possible dependence between entry times and loss to follow-up. We adapt and extend to the interim analysis setting the DB–MC approach of Tian et al. (Tian et al., 2022), originally developed in reliability engineering to construct prediction intervals for the number of future item failures. Prediction intervals are obtained as the quantiles of a parametric-bootstrap estimator of the conditional CMF of the future event count. Importantly, the parametric bootstrap is implemented conditional on the observed event and censoring indicators, thereby preserving the information available at the interim analysis.

The Poisson–binomial representation of the future event count provides a flexible way to model heterogeneous, subject-specific conditional probabilities of experiencing the event within the future time window, driven by staggered entry and, more generally, by covariate profiles. This formulation also naturally allows different parametric models for event times and censoring times. Embedding such models within the sampling scheme proposed is straightforward since it requires simulating event and loss to follow-up times from the chosen truncated parametric distributions. This yields substantial flexibility, leveraging a broad class of parametric survival models available in the literature (Crowther & Lambert, 2014; Liu et al., 2018). In this work we assumed a common dropout mechanism across covariate profiles, but the approach readily extends to settings where dropout also varies by covariates (e.g., treatment arm). The key requirement is that, conditional on the covariates, the event time and the loss-to-follow-up time are independent and their distributions share no parameters.

We examined the operating characteristics of the proposed method across a range of factors of interest in interim monitoring settings and with a case study on pediatric ALL. Follow-up maturity and prediction horizon emerged as key determinants of interval performance: more mature follow-up and shorter horizons led to better coverage, whereas longer horizons reduced coverage. Loss to follow-up produced modest reduction in coverage, which became more pronounced for longer prediction horizons. This reflects an information trade-off: while additional loss to follow-up can inform the censoring model, it simultaneously reduces the information for estimating the event-time distribution because fewer events are observed.

Across simulations, using more flexible parametric extensions of simpler models did not systematically improve prediction performance. This result aligns with those of Mori et al. (Mori et al., 2024). Although a more general model could be a safe choice if assumptions on the survival distribution are difficult to ascertain, the risk of overfitting should be considered in settings with low follow-up maturity, even when the proportion censored is small. The analysis of the real case suggests that model choice should be guided not only by information criteria but also by extrapolative behavior beyond the maximum follow-up observed at interim assessed via graphical inspection. Models implying different survival and hazard shapes may exhibit similar extrapolation, e.g., members of the log-location–scale family. The ability of the proposed framework to accommodate multiple parametric specifications also facilitates sensitivity analyses for predicted event counts under different distributions.

A further remark concerns the inferential perspective adopted in this work. In this work, inference is conditional on the realized interim dataset. In a frequentist setting, uncertainty is quantified by viewing the observed data as one realization from a hypothetical sequence of replications conducted under the same conditions. Here the same principle is applied to a future state of the same trial: the target is the distribution of what will be observed at a later calendar time, i.e., a within-sample prediction problem. This implicitly requires that the information available at the interim time is representative of what will be observed at later looks. The proposed bootstrap scheme is designed to mirror this perspective.

Further research could address the limitations underlying our approach and connect it to a set of active areas of research. First, we assume that the data at the interim analysis is free of reporting delays. In multicenter trials, however, delays in data entry and event reporting are common and can materially affect interim monitoring and prediction (Aubel et al., 2021; Tsiatis & Davidian, 2022; J. Wang et al., 2012). Extensions that explicitly account for delayed reporting would therefore be valuable. Second, we focus on settings in which accrual is complete at the prediction time. In many trials, interim analyses occur while recruitment is ongoing, so a practically relevant extension is joint prediction of both future accrual and future events as often considered in literature on time to endpoint maturation. Third, we assume access to unblinded, patient-level information. In practice, interim analyses are frequently conducted under blinding constraints to preserve trial integrity, limiting the availability of individual-level covariates or even treatment indicators. Related work on time to endpoint maturation prediction under blinded data (Donovan et al., 2006; Fu et al., 2025; H. Zhang et al., 2025) suggests promising directions to adapt our framework to blinded settings. Regarding the survival model, we restrict attention to regression-based parametric specifications without explicitly modeling potential violations of the covariates effect scale (e.g., departures from proportional hazards, proportional odds, or accelerated failure time assumptions). While in the motivating application ignoring such violations did not lead to marked differences in prediction intervals, the generalizability of this observation warrants further investigation. Lastly, our work may benefit from the extensive literature on parametric survival extrapolation from clinical trials for economic evaluation (E. Y. T. Chen et al., 2024; Cooper et al., 2022; Gray et al., 2021; Jackson, 2023; N. Latimer, 2011; N. R. Latimer & Adler, 2022; Palmer et al., 2023; Rutherford et al., 2020; Sweeting et al., 2023), where model choice and extrapolative performance are central concerns. Leveraging insights from this literature could be a promising avenue for future work.

## References

Akritis, M. G. (1986). Bootstrapping the kaplan-meier estimator. *Journal of the American Statistical Association*, 81(396), 1032–1038. <https://doi.org/10.1080/01621459.1986.10478369>

Anisimov, V., Gormley, S., Baverstock, R., & Kineza, C. (2021, August). Advanced models for predicting event occurrence in event-driven clinical trials accounting for patient dropout, cure and ongoing recruitment. <https://arxiv.org/abs/2108.09196>

Anisimov, V. V. (2011). Predictive event modelling in multicenter clinical trials with waiting time to response. *Pharmaceutical Statistics*, 10, 517–522. <https://doi.org/10.1002/pst.525>

Aubel, P., Antigny, M., Fougeray, R., Dubois, F., & Saint-Hilary, G. (2021). A bayesian approach for event predictions in clinical trials with time-to-event outcomes. *Statistics in Medicine*, 40(28), 6344–6359. <https://doi.org/10.1002/sim.9186>

Austin, P. C. (2023). The iterative bisection procedure: A useful tool for determining parameter values in data-generating processes in monte carlo simulations. *BMC Medical Research Methodology*, 23. <https://doi.org/10.1186/s12874-023-01836-5>

Bagiella, E., & Heitjan, D. F. (2001). Predicting analysis times in randomized clinical trials. *Statistics in Medicine*, 20, 2055–2063. <https://doi.org/10.1002/sim.843>

Baldi, I., Azzolina, D., Soriani, N., Barbetta, B., Vaghi, P., Giacovelli, G., Berchialla, P., & Gregori, D. (2020). Overrunning in clinical trials: Some thoughts from a methodological review. *Trials*, 21. <https://doi.org/10.1186/s13063-020-04526-5>

Barndorff-Nielsen, O. E., & Cox, D. R. (1996). Prediction and asymptotics. *Bernoulli*, 2(4), 319–340. <https://doi.org/10.2307/3318417>

Bender, R., Augustin, T., & Blettner, M. (2005). Generating survival times to simulate cox proportional hazards models. *Statistics in Medicine*, 24(11), 1713–1723. <https://doi.org/10.1002/sim.2059>

Beran, R. (1990). Calibrating prediction regions. *Source: Journal of the American Statistical Association*, 85, 37.

Bilker, W. B., & Wang, M. C. (1997). Bootstrapping left truncated and right censored data. *Communications in Statistics Part B: Simulation and Computation*, 26, 141–171. <https://doi.org/10.1080/03610919708813372>

Bjørnstad, J. F. (1990). Predictive likelihood: A review. *Source: Statistical Science*, 5, 242–254.

Brilleman, S. L., Wolfe, R., Moreno-Betancur, M., & Crowther, M. J. (2020). Simulating survival data using the simsurv r package. *Journal of Statistical Software*, 97(3), 1–27. <https://doi.org/10.18637/jss.v097.i03>

Cario, M. C., & Nelson, B. L. (1997). Modeling and generating random vectors with arbitrary marginal distributions and correlation matrix.

Chen, E. Y. T., Leontyeva, Y., Lin, C. N., Wang, J. D., Clements, M. S., & Dickman, P. W. (2024). Comparing survival extrapolation within all-cause and relative survival frameworks by standard parametric models and flexible parametric spline models using the swedish cancer registry. *Medical Decision Making*, 44, 269–282. <https://doi.org/10.1177/0272989X241227230>

Chen, T. T. (2016). Predicting analysis times in randomized clinical trials with cancer immunotherapy data analysis, statistics and modelling. *BMC Medical Research Methodology*, 16. <https://doi.org/10.1186/s12874-016-0117-3>

Conter, V., Valsecchi, M. G., Cario, G., Zimmermann, M., Attarbaschi, A., Starý, J., Niggli, F., Dalla Pozza, L., Elitzur, S., Silvestri, D., Locatelli, F., Mörck, A., Engstler, G., Smisek, P., Bodmer, N., Barbaric, D., Izraeli, S., Rizzari, C., Boos, J., ... Schrappe, M. (2024). Four additional doses of peg-l-asparaginase during the consolidation phase in the aieop-bfm all 2009 protocol do not improve outcome and increase toxicity in high-risk all: Results of a randomized study. *Journal of Clinical Oncology*, 42(8), 915–926. <https://doi.org/10.1200/JCO.23.01388>

Cooper, M., Smith, S., Williams, T., & Aguiar-Ibáñez, R. (2022). How accurate are the longer-term projections of overall survival for cancer immunotherapy for standard versus more flexible parametric extrapolation methods? *Journal of Medical Economics*, 25, 260–273. <https://doi.org/10.1080/13696998.2022.2030599>

Cox, C., Chu, H., Schneider, M. F., & Muñoz, A. (2007). Parametric survival analysis and taxonomy of hazard functions for the generalized gamma distribution. *Statistics in Medicine*, 26, 4352–4374. <https://doi.org/10.1002/sim.2836>

Crowther, M. J., & Lambert, P. C. (2013). Simulating biologically plausible complex survival data. *Statistics in Medicine*, 32(23), 4118–4134. <https://doi.org/10.1002/sim.5823>

Crowther, M. J., & Lambert, P. C. (2014). A general framework for parametric survival analysis. *Statistics in Medicine*, 33(30), 5280–5297. <https://doi.org/10.1002/sim.6300>

Donovan, J. M., Elliott, M. R., & Heitjan, D. F. (2006). Predicting event times in clinical trials when treatment arm is masked. *Journal of Biopharmaceutical Statistics*, 16, 343–356. <https://doi.org/10.1080/10543400600609445>

Efron, B. (1981). Censored data and the bootstrap. *Journal of the American Statistical Association*, 76(374), 312–319. <https://doi.org/10.1080/01621459.1981.10477650>

Fang, L., & Su, Z. (2011). A hybrid approach to predicting events in clinical trials with time-to-event outcomes. *Contemporary Clinical Trials*, 32, 755–759. <https://doi.org/10.1016/j.cct.2011.05.013>

Friede, T., Pohlmann, H., & Schmidli, H. (2019). Blinded sample size reestimation in event-driven clinical trials: Methods and an application in multiple sclerosis. *Pharmaceutical Statistics*, 18, 351–365. <https://doi.org/10.1002/pst.1927>

Fu, J., Zhao, D., Skanji, D., Liu, H., Tang, R. S., & Yuan, Y. (2025). Bayesian prediction of event times using mixture model for blinded randomized controlled trials. *Statistics in Medicine*, 44(28-30), e70310. <https://doi.org/10.1002/sim.70310>

Gasparini, A., & White, I. R. (2024). *Rsimsum: Analysis of simulation studies including monte carlo error* [R package version 0.13.0]. <https://doi.org/10.32614/CRAN.package.rsimsum>

Goodman, M. S., Li, Y., & Tiwari, R. C. (2011). Detecting multiple change points in piecewise constant hazard functions. *Journal of Applied Statistics*, 38, 2523–2532. <https://doi.org/10.1080/02664763.2011.559209>

Gray, J., Sullivan, T., Latimer, N. R., Salter, A., Sorich, M. J., Ward, R. L., & Karnon, J. (2021). Extrapolation of survival curves using standard parametric models and flexible parametric spline models: Comparisons in large registry cohorts with advanced cancer. *Medical Decision Making*, 41, 179–193. <https://doi.org/10.1177/0272989X20978958>

Gross, S. T., & Lai, T. L. (1996). Bootstrap methods for truncated and censored data. *Statistica Sinica*, 6(3), 509–530. <https://www.jstor.org/stable/24305605>

Hade, E. M., Jarjoura, D., & Wei, L. (2010). Sample size re-estimation in a breast cancer trial. *Clinical Trials*, 7, 219–226. <https://doi.org/10.1177/1740774510367525>

Hannig, J., Iyer, H., & Patterson, P. (2006). Fiducial generalized confidence intervals. *Journal of the American Statistical Association*, 101, 254–269. <https://doi.org/10.1198/016214505000000736>

Harris, I. R. (1989). Predictive fit for natural exponential families. 76, 675–684. <https://www.jstor.org/stable/2336627?seq=1&cid=pdf->

Heitjan, D. F., Ge, Z., & Ying, G. S. (2015, April). Real-time prediction of clinical trial enrollment and event counts: A review. <https://doi.org/10.1016/j.cct.2015.07.010>

Hess, K., & Gentleman, R. (2021). *Muhaz: Hazard function estimation in survival analysis* [R package version 1.2.6.4]. <https://doi.org/10.32614/CRAN.package.muhaz>

Hjort, N. L. (1985, November). *Bootstrapping cox's regression model* (Technical Report No. LCS 21 (also NSF-241)). Department of Statistics, Stanford University. <https://purl.stanford.edu/wv616sr1865>

Hong, Y. (2013). On computing the distribution function for the poisson binomial distribution. *Computational Statistics and Data Analysis*, 59, 41–51. <https://doi.org/10.1016/j.csda.2012.10.006>

Hong, Y., Meeker, W. Q., & McCalley, J. D. (2009). Prediction of remaining life of power transformers based on left truncated and right censored lifetime data. *Annals of Applied Statistics*, 3, 857–879. <https://doi.org/10.1214/00-AOAS231>

Hong, Y., & R Core Team. (2024). *Poibin: The poisson binomial distribution* [R package version 1.6]. <https://doi.org/10.32614/CRAN.package.poibin>

Jackson, C. H. (2023). Survextrap: A package for flexible and transparent survival extrapolation. *BMC Medical Research Methodology*, 23, 282. <https://doi.org/10.1186/s12874-023-02094-1>

Jackson, C. H. (2024). *Flexsurv: Flexible parametric survival and multi-state models* [R package version 2.3.2]. Retrieved January 6, 2026, from <https://CRAN.R-project.org/package=flexsurv>

Jennison, C., & Turnbull, B. W. (2025). *Group sequential and adaptive methods for clinical trials* (2nd ed.). Chapman; Hall/CRC. <https://doi.org/10.1201/9781584888482>

Jiang, S., Swanson, D., & Betensky, R. A. (2021). Estimation of the censoring distribution in clinical trials. *Contemporary Clinical Trials Communications*, 23. <https://doi.org/10.1016/j.conc.2021.100842>

Kim, K. (2014). Maximum duration and information trials. In N. Balakrishnan (Ed.), *Methods and applications of statistics in clinical trials, volume 1: Concepts, principles, trials, and designs* (pp. 515–521). John Wiley & Sons, Inc. <https://doi.org/10.1002/9781118596005.ch41>

Klein, J. P., & Moeschberger, M. L. (2003). *Survival analysis: Techniques for censored and truncated data* (2nd ed.). Springer. <https://doi.org/10.1007/b97377>

Lan, K. K. G., & Demets, D. L. (1989). Changing frequency of interim analysis in sequential monitoring. 45, 1017–1020. <https://www.jstor.org/stable/2531701>

Lan, Y., & Heitjan, D. F. (2018). Adaptive parametric prediction of event times in clinical trials. *Clinical Trials*, 15, 159–168. <https://doi.org/10.1177/1740774517750633>

Latimer, N. (2011, June). *Nice dsu technical support document 14: Survival analysis for economic evaluations alongside clinical trials – extrapolation with patient-level data* (Technical Support Document No. 14) (Last updated March 2013). Decision Support Unit (DSU), School of Health and Related Research (ScHARR), University of Sheffield. <http://www.nicedsu.org.uk>

Latimer, N. R., & Adler, A. I. (2022). Extrapolation beyond the end of trials to estimate long term survival and cost effectiveness. *BMJ Medicine*, 1, e000094. <https://doi.org/10.1136/bmjjmed-2021-000094>

Lawless, J. F., & Fredette, M. (2005). Frequentist prediction intervals and predictive distributions. 92, 529–542. <https://www.jstor.org/stable/20441212?seq=1&cid=pdf>

Liu, X., Pawitan, Y., & Clements, M. (2018). Parametric and penalized generalized survival models. *Statistical Methods in Medical Research*, 27(5), 1531–1546. <https://doi.org/10.1177/0962280216664760>

Machida, R., Sakamaki, K., Ohigashi, T., & Sozu, T. (2025). Dynamic prediction of analysis timing in clinical trials using joint models of longitudinal and time-to-event data. *Statistics in Medicine*, 44(28-30), e70312. <https://doi.org/10.1002/sim.70312>

Mee, R. W., & Kushary, D. (1994). Prediction limits for the weibull distribution utilizing simulation. *Computational Statistics & Data Analysis*, 17(3), 327–336. [https://doi.org/10.1016/0167-9473\(92\)00072-Y](https://doi.org/10.1016/0167-9473(92)00072-Y)

Meeker, W. Q., & Escobar, L. A. (1998). Statistical prediction based on censored life data. *Chapter*.

Meeker, W. Q., Hahn, G. J., & Escobar, L. A. (2017). *Statistical intervals: A guide for practitioners and researchers* (2nd ed.). John Wiley & Sons. <https://doi.org/10.1002/9781118594841>

Mori, T., Komukai, S., Hattori, S., & Friede, T. (2024). Flexible spline models for blinded sample size reestimation in event-driven clinical trials. *Pharmaceutical Statistics*. <https://doi.org/10.1002/pst.2459>

Ou, F. S., Heller, M., & Shi, Q. (2019). Milestone prediction for time-to-event endpoint monitoring in clinical trials. *Pharmaceutical Statistics*, 18, 433–446. <https://doi.org/10.1002/pst.1934>

Palmer, S., Borget, I., Friede, T., Husereau, D., Karnon, J., Kearns, B., Medin, E., Peterse, E. F. P., Klijn, S. L., Verburg-Baltussen, E. J. M., Fenwick, E., & Borrill, J. (2023). A guide to selecting flexible survival models to inform economic evaluations of cancer immunotherapies. *Value in Health*, 26(2), 185–192. <https://doi.org/10.1016/j.jval.2022.07.009>

Prentice, R. L. (1975). Discrimination among some parametric models. *Biometrika*, 62, 607. <https://about.jstor.org/terms>

Proschan, M. A., Follmann, D. A., & Waclawiw, M. A. (1992). Effects of assumption violations on type i error rate in group sequential monitoring. 48, 1131–1143. <https://www.jstor.org/stable/2532704>

R Core Team. (2025). *R: A language and environment for statistical computing* [Version 4.5.1]. R Foundation for Statistical Computing. Vienna, Austria. <https://www.R-project.org/>

Royston, P., & Parmar, M. K. (2002). Flexible parametric proportional-hazards and proportional-odds models for censored survival data, with application to prognostic modelling and estimation of treatment effects. *Statistics in Medicine*, 21, 2175–2197. <https://doi.org/10.1002/sim.1203>

Rufibach, K. (2025). *Eventtrack: Event prediction for time-to-event endpoints* [R package version 1.0.4]. Retrieved January 6, 2026, from <https://CRAN.R-project.org/package=eventTrack>

Rutherford, M. J., Lambert, P. C., Sweeting, M. J., Pennington, B., Crowther, M. J., Abrams, K. R., & Latimer, N. R. (2020, January). *Nice dsu technical support document 21: Flexible methods for survival analysis* (Technical Support Document No. 21) (Report date: 23 January 2020). Decision Support Unit (DSU), School of Health and Related Research (SCHARR), University of Sheffield. <http://www.nicedsu.org.uk>

Shen, J., Liu, R. Y., & ge Xie, M. (2018). Prediction with confidence—a general framework for predictive inference. *Journal of Statistical Planning and Inference*, 195, 126–140. <https://doi.org/10.1016/j.jspi.2017.09.012>

shuang Ying, G., Zhang, Q., Lan, Y., Li, Y., & Heitjan, D. F. (2017). Cure modeling in real-time prediction: How much does it help? *Contemporary Clinical Trials*, 59, 30–37. <https://doi.org/10.1016/j.cct.2017.05.012>

Stacy, E. W. (1962). A generalization of the gamma distribution. *The Annals of Mathematical Statistics*, 33, 1187–1192. <https://doi.org/10.1214/aoms/1177704481>

Sweeting, M. J., Rutherford, M. J., Jackson, D., Lee, S., Latimer, N. R., Hettle, R., & Lambert, P. C. (2023, August). Survival extrapolation incorporating general population mortality using excess hazard and cure models: A tutorial. <https://doi.org/10.1177/0272989X231184247>

Tang, W., & Tang, F. (2022). The poisson binomial distribution— old & new. *Statistical Science*, 38. <https://doi.org/10.1214/22-sts852>

Therneau, T. M. (2020). *Survival: Survival analysis* [R package version 3.2-7]. <https://CRAN.R-project.org/package=survival>

Tian, Q., Meng, F., Nordman, D. J., & Meeker, W. Q. (2022). Predicting the number of future events. *Journal of the American Statistical Association*, 117, 1296–1310. <https://doi.org/10.1080/01621459.2020.1850461>

Todd, S., Valdés-Márquez, E., & West, J. (2012, March). A practical comparison of blinded methods for sample size reviews in survival data clinical trials. <https://doi.org/10.1002/pst.516>

Tsiatis, A. A., & Davidian, M. (2022). Group sequential methods for interim monitoring of randomized clinical trials. *Statistics in Medicine*, 41, 5517–5536. <https://doi.org/10.1002/sim.9580>

Wang, C. M., Hannig, J., & Iyer, H. K. (2012). Fiducial prediction intervals. *Journal of Statistical Planning and Inference*, 142, 1980–1990. <https://doi.org/10.1016/j.jspi.2012.02.021>

Wang, J., Ke, C., Jiang, Q., Zhang, C., & Snapinn, S. (2012). Predicting analysis time in event-driven clinical trials with event-reporting lag. *Statistics in Medicine*, 31(9), 801–811. <https://doi.org/10.1002/sim.4506>

Wang, L., Liu, Y., Chen, X., & Pulkstenis, E. (2022). Real time monitoring and prediction of time to endpoint maturation in clinical trials. *Statistics in Medicine*, 41(18), 3596–3611. <https://doi.org/10.1002/sim.9436>

Wassmer, G., & Brannath, W. (2025). *Group sequential and confirmatory adaptive designs in clinical trials* (2nd ed.). Springer. <https://doi.org/10.1007/978-3-031-89669-9>

Whitehead, J. (1992). Overrunning and underrunning in sequential clinical trials. *Controlled Clinical Trials*, 13(2), 106–121. [https://doi.org/10.1016/0197-2456\(92\)90017-T](https://doi.org/10.1016/0197-2456(92)90017-T)

Whitehead, J. (2001). Predicting the duration of sequential survival studies. *Drug Information Journal*, 35, 1387–1400.

Wu, J. (2018). *Statistical methods for survival trial design: With applications to cancer clinical trials using r*. CRC Press. <https://doi.org/10.1201/9780429470172>

Ying, G. S., & Heitjan, D. F. (2008). Weibull prediction of event times in clinical trials. *Pharmaceutical Statistics*, 7, 107–120. <https://doi.org/10.1002/pst.271>

Ying, G. S., & Heitjan, D. F. (2013). Prediction of event times in the rematch trial. *Clinical Trials*, 10, 197–206. <https://doi.org/10.1177/1740774512470314>

Ying, G.-S., Heitjan, D. F., & Chen, T.-T. (2004). Nonparametric prediction of event times in randomized clinical trials. *Clinical Trials*, 1(4), 352–361.

Zhang, H., Pu, J., Deng, S., Roychoudhury, S., Chu, H., & Robinson, D. (2025). Study duration prediction for clinical trials with time-to-event endpoints accounting for heterogeneous population [Epub 2025-04-20]. *Journal of Biopharmaceutical Statistics*, 35(6), 1255–1270. <https://doi.org/10.1080/10543406.2025.2489294>

Zhang, X., & Long, Q. (2012). Joint monitoring and prediction of accrual and event times in clinical trials. *Biometrical Journal*, 54, 735–749. <https://doi.org/10.1002/bimj.201100180>

## 7 Appendix

### 7.1 Prediction intervals methods

There are different ways to determine a prediction interval. In a Bayesian framework, the prediction intervals are recovered as the appropriate quantile of the posterior predictive density of  $Y$  (Geisser, 1993; Atchison, 1975). In a frequentist framework, the prediction is approached by calculating the probability that a future random observation  $Y$  falls in a random region which depends on  $\mathcal{D}$

$$P(Y \in R(\mathcal{D}) \mid \varphi(\boldsymbol{\vartheta})) = 1 - \alpha. \quad (16)$$

The random region  $R(\mathcal{D})$  defines the prediction interval, that is,  $R(\mathcal{D}) = \text{PI}_{1-\alpha}(\mathcal{D})$ , and  $\varphi(\boldsymbol{\vartheta})$  are the common parameters of the joint distribution of  $Y$  and  $\mathcal{D}$ . Frequentist-based prediction intervals approaches for discrete predictand generally fall in two different methodology. The first class of methods is that of prediction intervals recovered from a pivotal quantity, e.g. a location-scale transformation. A general construction uses the probability integral transform (Lawless and Fredette, 2005). Since  $U = F_Y(Y \mid \mathcal{D}; \varphi(\boldsymbol{\vartheta})) \sim \text{Uniform}(0, 1)$ , hence prediction bounds are taken such that  $P(u_{\alpha/2} \leq U \leq u_{1-\alpha/2}) = 1 - \alpha$ . When no exact pivotal quantity exists, one may use an approximate pivotal quantity  $\tilde{U}(\mathcal{D}, Y) \xrightarrow{d} \text{Uniform}(0, 1)$  which yields the asymptotic interval  $\text{PI}_{1-\alpha}(\mathbf{D}) = \{y : \tilde{u}_{\alpha/2} \leq \tilde{U}(\mathbf{D}, Y) \leq \tilde{u}_{1-\alpha/2}\}$  provided that  $\varphi(\hat{\boldsymbol{\theta}})$  is a consistent estimator of  $\varphi(\boldsymbol{\vartheta})$ . The plug-in approach sets  $\tilde{u}_{\alpha/2} = \alpha/2$  and  $\tilde{u}_{1-\alpha/2} = 1 - \alpha/2$ . However, coverage can deviate from nominal because  $\hat{\boldsymbol{\theta}}$  is treated as fixed (Beran, 1990). Calibration may improve the coverage of the plug-in prediction interval when no exact pivotal quantity exists. Since for the plug-in prediction intervals  $P(Y \in \text{PI}_{1-\alpha}(\mathcal{D}) \mid \varphi(\boldsymbol{\vartheta})) \leq 1 - \alpha$ , the goal of calibration is to find  $\gamma$  such that  $P(Y \in \text{PI}_{1-\gamma}(\mathcal{D}) \mid \varphi(\boldsymbol{\vartheta})) = 1 - \alpha$ , and then take  $\tilde{u}_{\gamma/2}$  and  $\tilde{u}_{1-\gamma/2}$  as prediction bounds. The function that map  $\alpha \mapsto \gamma$  is generally unknown, it can be obtained by asymptotic expansion (Barndorff-Nielsen & Cox, 1996) or simulation (Beran, 1990).

The second class of methods relies on predictive distribution defined in a non-Bayesian setting (Bjørnstad, 1990). Harris (Harris, 1989) proposed approximating the integral in the posterior predictive by marginalizing the conditional CDF/CMF over  $\varphi(\boldsymbol{\vartheta})$  replacing the posterior of  $\varphi(\boldsymbol{\vartheta})$  with the sampling distribution of an estimator  $\varphi(\hat{\boldsymbol{\theta}})$  for the fixed parameter  $\varphi(\boldsymbol{\vartheta})$ , i.e.  $p(\varphi(\hat{\boldsymbol{\theta}}) \mid \mathbf{D}; \varphi(\boldsymbol{\vartheta}))$ . Thus, the resulting predictive CDF has the form:

$$\mathcal{F}_Y(y \mid \mathbf{D}) = \int F_Y(y \mid \mathbf{D}; \varphi(\boldsymbol{\vartheta})) p(\varphi(\hat{\boldsymbol{\theta}}) \mid \mathbf{D}; \varphi(\boldsymbol{\vartheta})) d\varphi(\hat{\boldsymbol{\theta}}) \quad (17)$$

If the integral has no closed-form solution or  $p(\varphi(\hat{\boldsymbol{\theta}}) \mid \mathbf{D}; \varphi(\boldsymbol{\vartheta}))$  cannot be derived analytically, Harris (1989) proposed approximating the sampling distribution of  $\varphi(\hat{\boldsymbol{\theta}})$  by its parametric bootstrap counterpart. Since

$$\int F_Y(y \mid \mathbf{D}; \varphi(\boldsymbol{\vartheta})) p(\varphi(\hat{\boldsymbol{\theta}}) \mid \mathbf{D}; \varphi(\boldsymbol{\vartheta})) d\varphi(\hat{\boldsymbol{\theta}}) = \mathbb{E}_{\hat{\boldsymbol{\Theta}}}[F_Y(y \mid \mathbf{D}; \varphi(\boldsymbol{\theta}))], \quad (18)$$

the bootstrap conditional CDF/CMF is

$$\hat{F}_Y^*(y \mid \mathbf{D}) = \frac{1}{B} \sum_{b=1}^B F_Y(y \mid \mathbf{D}_b^*; \varphi(\hat{\boldsymbol{\theta}}_b^*)) \quad (19)$$

$$= \hat{\mathbb{E}}_{\varphi(\hat{\boldsymbol{\theta}})}[F_Y(y \mid \mathbf{D}; \varphi(\boldsymbol{\vartheta}))], \quad (20)$$

where  $\varphi(\hat{\boldsymbol{\theta}}_1^*), \dots, \varphi(\hat{\boldsymbol{\theta}}_B^*)$  are realized bootstrap version of  $\varphi(\hat{\boldsymbol{\theta}})$  obtained on the bootstrap sample  $\mathbf{D}_b^*$  and the expectation is taken with respect to the distribution of  $\varphi(\hat{\boldsymbol{\theta}})$  induced by the bootstrap. By the law of large numbers,  $\mathcal{F}_Y^*(y \mid \mathbf{D})$  consistently estimates the conditional distribution of  $Y$ . Note that  $\mathcal{F}_Y^*(y \mid \mathbf{D})$  is conceptually different from the posterior predictive density in the Bayesian framework since  $\mathcal{F}_Y^*(y \mid \mathbf{D})$  is a *sample-based estimator* of a predictive CDF, not a probability distribution in its own right (Lawless & Fredette, 2005). Harris (Harris, 1989) showed that the bootstrap predictive CDF is asymptotically superior to the plug-in method in terms of Kullback-Leibler divergence for the natural exponential family.

### 7.2 The Poisson-binomial Distribution

The Poisson Binomial distribution is the distribution of the sum of independent but not identically distributed random indicator. Each indicator is a Bernoulli random variable and the individual success probabilities vary. A special case of the Poisson-Binomial distribution is the ordinary Binomial distribution when all success probabilities are equal.

Let  $\zeta_j$  be a series of independent and non-identically distributed random indicators. In particular,  $\zeta_j \sim \text{Bernoulli}(\pi_j)$  where  $\pi_j = P(\zeta_j = 1)$  is the success probability of indicator  $j$  and not all  $\pi_j$ 's are equal. The Poisson-Binomial random variable  $Y$  is defined as the sum of independent and non-identically distributed random indicators, i.e.,  $Y = \sum_j \zeta_j$ .  $Y$  can take values in  $\{0, 1, 2, \dots, n\}$

Let  $f_Y(y) = P(Y = y)$  be the probability mass function (PMF) for the Poisson binomial random variable  $Y$ , and let  $F_Y(y) = P(Y \leq y)$ , the probability of having at most  $y$  successes out of a total of  $n$ , i.e., the cumulative density function (cdf). The analytical expression of the pmf and the cdf of the Poisson-Binomial distribution are the following (Tang & Tang, 2022):

$$f(y) = \sum_{A \in \Omega} \prod_{k \in A} p_k \prod_{k' \in A^c} (1 - p_{k'}) \quad F(y) = \sum_{n=0}^y f(n) ,$$

where  $\Omega$  is the set of all subsets of  $y$  integers that can be selected from  $n$  and  $A^c$  is the complement of  $A$ . Note that  $\Omega$  will contain  $n!((n-y)!y!)$ . To compute  $f(y)$  and  $F(y)$ , it is needed to enumerate all elements in  $\Omega$ , which is not practical even when  $n$  is small (e.g.,  $n = 30$ ). Thus, computing  $f(y)$  and  $F(y)$  is not straightforward. Approximation methods such as the Poisson approximation and Normal approximations have been used in literature (e.g., (Hong et al., 2009)), but connections with others distributions are possible. See the paper of Tang et al. (Tang & Tang, 2022) for an in-depth review of the properties of the Poisson-binomial distribution.

### 7.3 Derivation of $\pi_j$ and special cases

For patient  $j$ , let  $T_j$  denote the event time with pdf  $f_{\theta}(t | \mathbf{z}_j)$  and cdf  $F_{\theta}(t | \mathbf{z}_j)$ , where  $\mathbf{z}_j$  is a vector of individual covariates. Let  $C_j = \min(L_j, \tau_j)$  denote the censoring time, where  $L_j$  is the random time to loss to follow-up with marginal PDF  $\tilde{g}_{\psi}$  and CDF  $\tilde{G}_{\psi}$ , and  $\tau_j = t_c - \tau_{aj}$  is the subject-specific interim censoring time, induced by the common interim calendar time  $t_c$  and the entry time  $\tau_{aj}$ . For a patient still at risk at  $t_c$ , we define the conditional probability of experiencing the event of interest within the prediction window  $(\tau_j, \tau_j + \Delta t]$ , given being at risk at the interim time  $t_c$ , as:

$$\begin{aligned} \pi_j &= \Pr(T_j \leq \min(\tau_j + \Delta t, L_j) \mid \gamma_j = 1, \mathbf{z}_j) \\ &= \Pr(T_j \leq \min(\tau_j + \Delta t, L_j) \mid \tau_j < \min(T_j, L_j), \mathbf{z}_j) \\ &= \frac{\Pr(\tau_j < T_j \leq \tau_j + \Delta t, T_j \leq L_j, \mathbf{z}_j)}{\Pr(T_j > \tau_j, L_j > \tau_j)}. \end{aligned}$$

Since we are conditioning on the time of individual interim censoring  $\tau_j$  and  $T_j \perp L_j$ , the numerator is:

$$\begin{aligned} \Pr(\tau_j < T_j \leq \tau_j + \Delta t, T_j \leq L_j, \mathbf{z}_j) &= \int_{\tau_j}^{\tau_j + \Delta t} f_{\theta}(u | \mathbf{z}_j) \{1 - \tilde{G}_{\psi}(u)\} du \\ &= \int_{\tau_j}^{\tau_j + \Delta t} f_{\theta}(u | \mathbf{z}_j) du - \int_{\tau_j}^{\tau_j + \Delta t} \tilde{G}_{\psi}(u) f_{\theta}(u | \mathbf{z}_j) du \\ &= [F_{\theta}(\Delta t + \tau_j | \mathbf{z}_j) - F_{\theta}(\tau_j | \mathbf{z}_j)] - \int_{\tau_j}^{\tau_j + \Delta t} \tilde{G}_{\psi}(u) f_{\theta}(u | \mathbf{z}_j) du, \end{aligned}$$

and the denominator:

$$\Pr(T_j > \tau_j, L_j > \tau_j) = [1 - F_{\theta}(\tau_j)] [1 - \tilde{G}_{\psi}(\tau_j)]$$

#### 7.3.1 Special cases and closed forms

**Exponential event time and censoring time distribution.** Consider the integral term in the expression

$$I_j = \int_{\tau_j}^{\tau_j + \Delta t} \tilde{G}_{\psi}(u | \psi) f_{\theta}(u | \mathbf{z}_j) du$$

. If event times are exponentially distributed with rate  $\lambda_{\mathbf{z}_j}$  depending on a vector of covariate and loss to follow-up time are exponential with rate  $\psi$ , then the integral is:

$$I_j = \int_{\tau_j}^{\Delta t + \tau_j} (1 - \exp[-\psi u]) \lambda_{\mathbf{z}_j} \exp[-\lambda_{\mathbf{z}_j} u] du$$

We separate the two components:

$$I_j = \underbrace{\int_{\tau_j}^{\Delta t + \tau_j} \lambda_{z_j} \exp[-(\lambda_{z_j} u)] du}_{A} - \underbrace{\int_{\tau_j}^{\Delta t + \tau_j} \exp[-\psi u] \lambda_{z_j} \exp[-(\lambda_{z_j} u)] du}_{B}.$$

The first term is:

$$A = F_{\theta}(\tau_j + \Delta t | z_j) - F_{\theta}(\tau_j | z_j) = \exp[-\lambda_{z_j} \tau_j] - \exp[-\lambda_{z_j} (\tau_j + \Delta t)]$$

The second term is:

$$\begin{aligned} B &= \frac{\lambda_{z_j}}{\lambda_{z_j} + \psi} \{ \exp[-(\lambda_{z_j} + \psi) t_{c_j}] - \exp[-(\lambda_{z_j} + \psi) (t_{c_j} + \Delta t)] \} \\ &= \frac{\lambda_{z_j}}{\lambda_{z_j} + \psi} \exp[-(\lambda_{z_j} + \psi) t_{c_j}] (1 - \exp[-(\lambda_{z_j} + \psi) \Delta t]) \end{aligned}$$

. Since:

$$\begin{aligned} \Pr(T_j > t_{c_j}, L_j > t_{c_j}) &= [1 - F_{\theta}(t_{c_j})] [1 - \tilde{G}_{\psi}(t_{c_j})] \\ &= \exp(-\lambda_{z_j} t_{c_j}) \exp(-\psi t_{c_j}) \\ &= \exp[-(\lambda_{z_j} + \psi) t_{c_j}]. \end{aligned}$$

Thus:

$$\pi_j = \frac{\lambda_{z_j} (1 - \exp[-(\lambda_{z_j} + \psi) \Delta t])}{\lambda_{z_j} + \psi}.$$

This expression was presented for the first time in Biagella and Heijan (Bagiella & Heijan, 2001) and used by Friede et al. (Friede et al., 2019) for sample size re-estimation. Anisimov et al. (V. Anisimov et al., 2021) extended this expression in the presence of a cure fraction, both under exponential and Weibull event time distribution.

**No random censoring (interim censoring only at  $t_c$ ).**

$$\pi_j = \frac{F_{\theta}(\tau_j + \Delta t) - F_{\theta}(\tau_j)}{1 - F_{\theta}(\tau_j + \Delta t)} = 1 - \frac{S_{\theta}(\tau_j + \Delta t)}{S_{\theta}(\tau_j)} = 1 - \exp(H_{\theta}(\tau_j) - H_{\theta}(\tau_j + \Delta t))$$

**No random censoring (interim censoring only at  $t_c$ ) and exponential event time distribution.**

$$\pi_j = 1 - \exp \left\{ \lambda_{z_j} \tau_j - \lambda_{z_j} (\tau_j + \Delta t) \right\} = 1 - \exp \left\{ -\lambda_{z_j} \Delta t \right\}$$

## 7.4 Likelihood Functions and Conditional PDF

Prior observing the interim data  $\mathbf{D}$ ,  $(T_j^{\text{obs}}, \delta_j, \varepsilon_j, \gamma_j)_{j=1}^n$  are random variables with joint PDF  $\Pr_{\boldsymbol{\vartheta}}(T_j^{\text{obs}}, \delta_j, \varepsilon_j, \gamma_j \mid \mathbf{z}_j)$ , where  $\boldsymbol{\vartheta} = (\boldsymbol{\theta}, \boldsymbol{\psi}, \boldsymbol{\phi})$  and  $(\boldsymbol{\theta}, \boldsymbol{\psi}, \boldsymbol{\phi}) \in \Theta \times \Psi \times \Phi$ .

Since  $\delta_j = 1 \Leftrightarrow (\varepsilon_j = 0, \gamma_j = 0)$  and  $\varepsilon_j = 1 \Leftrightarrow (\delta_j = 0, \gamma_j = 0)$  we can write the joint PDF as:

$$\begin{aligned} \Pr(T_j^{\text{obs}} = t, \delta_j, \varepsilon_j \mid \mathbf{z}_j) &= \prod_{j=1}^n \left[ f_{\boldsymbol{\theta}}(t \mid \mathbf{z}_j) \underbrace{\int_{l>t} \int_{\tau>t} g_{\boldsymbol{\psi}, \boldsymbol{\phi}}(l, \tau) d\tau dl}_{\Pr(L_j > t, \mathcal{T}_j > t) = \Pr(C_j > t)} \right]^{\delta_j} \\ &\times \left[ \{1 - F_{\boldsymbol{\theta}}(t \mid \mathbf{z}_j)\} \underbrace{\int_{\tau>t} g_{\boldsymbol{\psi}, \boldsymbol{\phi}}(l, \tau) d\tau}_{\Pr(L_j \in dt, \mathcal{T}_j > t)} \right]^{\varepsilon_j} \\ &\times \left[ \{1 - F_{\boldsymbol{\theta}}(t \mid \mathbf{z}_j)\} \underbrace{\int_{l>t} g_{\boldsymbol{\psi}, \boldsymbol{\phi}}(l, \tau) dl}_{\Pr(L_j > t, \mathcal{T}_j \in dt)} \right]^{1-\delta_j-\varepsilon_j}. \end{aligned}$$

Assuming  $T_j \perp C_j$  the likelihood for  $\boldsymbol{\theta}$  is

$$\begin{aligned} \mathcal{L}(\boldsymbol{\theta}) &\propto \prod_{j=1}^n \left[ f_{\boldsymbol{\theta}}(t \mid \mathbf{z}_j) \right]^{\delta_j} \left[ 1 - F_{\boldsymbol{\theta}}(t \mid \mathbf{z}_j) \right]^{\varepsilon_j} \left[ 1 - F_{\boldsymbol{\theta}}(t \mid \mathbf{z}_j) \right]^{1-\delta_j-\varepsilon_j} \\ &\propto \prod_{j=1}^n \left[ f_{\boldsymbol{\theta}}(t \mid \mathbf{z}_j) \right]^{\delta_j} \left[ 1 - F_{\boldsymbol{\theta}}(t \mid \mathbf{z}_j) \right]^{1-\delta_j}. \end{aligned}$$

Moreover, putting  $g_{\boldsymbol{\psi}, \boldsymbol{\phi}}(l, \tau) = \tilde{g}_{\boldsymbol{\psi}}(l) r_{\boldsymbol{\phi}}(\tau \mid l)$  the likelihood for  $\boldsymbol{\psi}$  is

$$\begin{aligned} \mathcal{L}(\boldsymbol{\psi}) &\propto \prod_{j=1}^n \left[ \int_{l>t} \tilde{g}_{\boldsymbol{\psi}}(l) dl \int_{\tau>t} r_{\boldsymbol{\phi}}(\tau \mid l) d\tau \right]^{\delta_j} \left[ \tilde{g}_{\boldsymbol{\psi}}(t) \int_{\tau>t} r_{\boldsymbol{\phi}}(\tau \mid l) d\tau \right]^{\varepsilon_j} \left[ r_{\boldsymbol{\phi}}(\tau \mid l) \int_{l>t} \tilde{g}_{\boldsymbol{\psi}}(l) dl \right]^{1-\delta_j-\varepsilon_j} \\ &\propto \prod_{j=1}^n \left[ \int_{l>t} \tilde{g}_{\boldsymbol{\psi}}(l) dl \right]^{\delta_j} \left[ \tilde{g}_{\boldsymbol{\psi}}(t) \right]^{\varepsilon_j} \left[ \int_{l>t} \tilde{g}_{\boldsymbol{\psi}}(l) dl \right]^{1-\delta_j-\varepsilon_j} \\ &\propto \prod_{j=1}^n \left[ \tilde{g}_{\boldsymbol{\psi}}(l) \right]^{\varepsilon_j} \left[ 1 - \tilde{G}_{\boldsymbol{\psi}}(l) \right]^{1-\varepsilon_j}. \end{aligned}$$

### 7.4.1 Conditional distribution (truncation)

Once we observe  $\mathbf{D} = (T_j^{\text{obs}}, \delta_j, \varepsilon_j, \gamma_j)_{j=1}^n$  at the interim time, conditioning on  $\mathcal{T}_j = \tau_j$  the PDF of  $T_j^{\text{obs}} \mid \delta_j = 1, \mathbf{z}_j$  is

$$\Pr(T_j^{\text{obs}} = t \mid \delta_j = 1, \mathbf{z}_j) = f_{\boldsymbol{\theta}}(t \mid t \leq \tau_j, \mathbf{z}_j) = \frac{f_{\boldsymbol{\theta}}(t \mid \mathbf{z}_j)}{F_{\boldsymbol{\theta}}(\tau_j, \mathbf{z}_j)}.$$

Conditional on  $\delta_j = 1$ , we have  $T_j^{\text{obs}} = T_j$ . Furthermore, conditioning on the subject-specific maximum follow-up time  $\tau_j$  restricts the support of  $T_j$  to  $(0, \tau_j]$ , i.e., the distribution of  $T_j$  is truncated at  $\tau_j$ . Same considerations hold for the PDF of  $T_j^{\text{obs}} \mid \varepsilon_j = 1, \mathbf{z}_j$ .

## 7.5 Parametric Bootstrap Sampling Scheme for the Approximation of the conditional CMF

---

**Algorithm 1:** Parametric bootstrap sampling scheme for approximating the conditional CMF

---

**Input:** Observed interim data  $\mathbf{D}$ ; interim time  $t_c$ ; entry dates  $\tau_{aj}$ ; prediction horizon  $\Delta t$ ; number of bootstrap replications  $B$ .

**Output:** Bootstrap estimator of the conditional CMF.

```

/* Step 1 */  

compute the ML estimates  $\hat{\theta}$  and  $\hat{\psi}$ ;  

/* Step 2 */  

obtain bootstrap replicates  $\mathbf{D}_b^*$  of the observed data:  

  for  $b \leftarrow 1$  to  $B$  do
    for  $j : \delta_j = 1$  do
      set  $\tau_j = t_c - \tau_{aj}$ ;  

      sample  $T_{jb}^* \sim f_{\hat{\theta}}(t \mid t \leq \tau_j, \mathbf{z}_j)$ ;  

      set  $T_{jb}^{\text{obs}} = T_{jb}^*$ ;  

    for  $j : \varepsilon_j = 1$  do
      set  $\tau_j = t_c - \tau_{aj}$ ;  

      sample  $L_{jb}^* \sim g_{\hat{\psi}}(t \mid t \leq \tau_j)$ ;  

      set  $T_{jb}^{\text{obs}} = L_{jb}^*$ ;  

    for  $j : \gamma_j = 1$  do
      set  $\tau_j = t_c - \tau_{aj}$ ;  

      set  $T_{jb}^{\text{obs}} = \tau_j$ ;  

  /* Step 3 */  

  compute the bootstrap ML estimates  $\hat{\theta}_b^*$  and  $\hat{\psi}_b^*$  on  $\mathbf{D}_b^* = (T_{jb}^{\text{obs}}, \delta_j, \varepsilon_j, \gamma_j, \mathbf{z}_j)_{j=1}^n$ ;  

  compute  $\pi_{jb}^*$  at a future prediction horizon  $\Delta t$  for only interim censored patients;  

/* Step 4 */  

for  $y \in \{0, \dots, n - \sum_j (\delta_j + \varepsilon_j)\}$  do
   $\hat{F}_Y^*(y \mid \mathbf{D}) = \frac{1}{B} \sum_{b=1}^B F_Y(y \mid \mathbf{D}_b^*; \hat{\pi}_b^*)$ ;  

return  $\hat{F}_Y^*(y \mid \mathbf{D})$ 

```

---

### 7.5.1 Sampling from the conditional/truncated density via inverse transform.

To generate times from a distribution truncated in  $(0, \tau]$ , one draws  $U \sim \text{Unif}(0, 1)$  and set  $T^* = F_{\theta}^{-1}(UF(\tau))$ . Equivalently, one can draw  $U \sim \text{Unif}(0, F(\tau))$  and set  $T^* = F_{\theta}^{-1}(U)$ . Since covariates are also included, it is possible to exploit the covariates effect scale, i.e., the way the vector of covariates  $\mathbf{z}$  acts on a baseline function of time. Here we review the strategy we adopted for some specialized cases.

**Proportional Hazard (PH) models.** Under PH assumption  $S_{\theta}(t \mid \mathbf{z}) = [S_{\theta}(t)]^{\eta(\mathbf{z})}$ , where  $S_{\theta}(t)$  is the baseline survival function and  $\eta(\mathbf{z}) = \text{HR}$  is the hazard ratio as function of the covariates and constant over time. Thus, times can be sampled from

$$T^* = F_{\theta}(U^{\dagger}), \quad U^{\dagger} = 1 - [1 - (UF_{\theta}(\tau \mid \mathbf{z}))]^{1/\text{HR}}, \quad U \sim \text{Unif}(0, 1).$$

This avoids drawing event times directly from  $F_{\theta}(t \mid \mathbf{z})$  when inverse sampling is not convenient, e.g. Royston-Parmar model with link function  $g(S(t)) = \log(-\log(S(t)))$ .

**Proportional Odds (PO) models.** Under PO assumption  $\log[1 - S_{\theta}(t \mid \mathbf{z})/S_{\theta}(t \mid \mathbf{z})] = \eta(\mathbf{z}) \log[1 - S_{\theta}(t)/S_{\theta}(t)]$ , where  $\log[1 - S_{\theta}(t)/S_{\theta}(t)]$  is the baseline odds and  $\eta(\mathbf{z}) = \text{OR}$  is the odds ratio as function of the covariates and constant over time. Thus, times can be sampled from

$$T^* = F_{\theta}(U^{\dagger}), \quad U^{\dagger} = 1 - \text{expit}[\text{logit}(1 - UF_{\theta}(\tau \mid \mathbf{z})) - \text{logit}(\text{OR})], \quad U \sim \text{Unif}(0, 1).$$

where  $\text{expit}(a) = 1/[1 + \exp(-a)]$  and  $\text{logit}(a) = \text{expit}^{-1}(a)$ . This avoids drawing event times directly from  $F_{\theta}(t \mid \mathbf{z})$  when inverse sampling is not convenient, e.g. Royston-Parmar model with link function  $g(S(t)) = \text{logit}(S(t))$ .

**Linear Probit (LP) models.** Under LP assumption  $\Phi^{-1}[1 - S_{\theta}(t | \mathbf{z})] = g(\mathbf{z}) \Phi^{-1}[1 - S_{\theta}(t)]$ , where  $\Phi^{-1}(\cdot)$  is the CDF of the standard normal distribution and  $\eta(\mathbf{z})$  is the linear predictor. Thus, times can be sampled from

$$T^* = F_{\theta}(U^{\dagger}), \quad U^{\dagger} = \Phi\left\{\Phi^{-1}[UF_{\theta}(\tau | \mathbf{z})] - \eta(\mathbf{z})\right\}, \quad U \sim \text{Unif}(0, 1).$$

This avoids drawing event times directly from  $F_{\theta}(t | \mathbf{z})$  when inverse sampling is not convenient, e.g. Royston-Parmar model with link function  $g(S(t)) = \text{probit}(S(t))$ .

## 7.6 Simulations general set-up and further results

Let  $Z$  denote a binary treatment indicator, with  $Z \sim \text{Bernoulli}(0.5)$  corresponding to equal allocation (1:1) between control ( $Z = 0$ ) and treatment ( $Z = 1$ ). Let  $T$  be the event time. Conditional on  $Z$ , the hazard function follows a Weibull proportional hazards model

$$h(t | Z) = h_0(t) \exp(\beta Z), \quad h_0(t) = \gamma \lambda_0 t^{\gamma-1} \quad t > 0,$$

so that  $T | Z \sim \text{Weibull}(\gamma, \lambda^*)$ , with  $\lambda^* = \lambda_0 \exp(\beta Z)$ . We call here  $\lambda^*$  as the scale and  $\gamma$  as the shape of the Weibull distribution. For each subject, we simulated the time-to-event outcome thanks to the probability integral transform by evaluating the quantile function of the Weibull distribution,

$$\left(\frac{-\log(U)}{\lambda^*}\right)^{1/\gamma},$$

where  $U \sim \text{Unif}(0, 1)$  (Bender et al., 2005). For both data-generating mechanisms, we fixed  $\gamma = 0.6$  and calibrated the baseline scale parameter  $\lambda_0$  to achieve the target proportion of interim censoring under a specified hazard ratio (i.e., with  $\exp(\beta Z)$  held fixed). See section 7.6.1 and 7.6.2.

We generated staggered entry dates and loss to follow-up time with the NORTA sampling (Carlo & Nelson, 1997) to ensure correlated distributions with separate parameters. The NORTA (NORmal To Anything) sampling is as follows. Let

$$(Z_1, Z_2)^{\top} \sim \mathcal{N}\left(\mathbf{0}, \begin{pmatrix} 1 & \rho^* \\ \rho^* & 1 \end{pmatrix}\right),$$

where  $\rho^* \in (-1, 1)$  is an *auxiliary* correlation. Define

$$U_1 = \Phi(Z_1), \quad U_2 = \Phi(Z_2),$$

so that  $U_1, U_2 \sim \text{Unif}(0, 1)$  with dependence induced by  $\rho^*$ . Then obtain the target marginals via inverse-CDF transforms as

$$\mathcal{T} = \tau_a U_1 \sim \text{Unif}(0, \tau_a), \quad L = F_{\text{Exp}(\psi)}^{-1}(U_2) = -\frac{\log(U_2)}{\psi} \sim \text{Exp}(\psi).$$

independent of  $(T, Z)$ , where  $\tau_a$  denotes the maximum entry dates admissible, i.e. accrual's end. Then, interim censoring time  $\mathcal{T}$  are taken as  $\mathcal{T} = t_c - \tau_a$ , where  $t_c$  is the interim time and  $\tau_a = 3$  for both data generating mechanism.  $\rho^*$  is chosen so that  $\text{Corr}(\mathcal{T}, L) = \rho$ . Since the mapping  $\rho^* \mapsto \rho$  is not linear and has no closed form here, we calibrate  $\rho^*$  numerically with bisection, by repeatedly simulating  $(\mathcal{T}, L)$  for a candidate  $\rho$  and updating  $\rho^*$  until the empirical correlation matches the target  $\rho$  within a prescribed tolerance (See manuscript). Here,  $\psi = k\lambda_0$ , where  $\lambda_0$  is the baseline scale of the Weibull recovered with the bisection procedure.

Finally,  $T_j^{\text{obs}} = \min(T, L, \mathcal{T})$  and indicators are obtained accordingly. In the case of only interim censoring, loss to follow-up times are not simulated and then  $T_j^{\text{obs}} = \min(T, \mathcal{T})$ .

### 7.6.1 Data-generating mechanisms - $\mathcal{S}_1$

1. Fix the design values of the simulation  $\Delta t, t_c, \rho, HR, k$ .
2. Find with the bisection procedure the value of  $\lambda_0$  that ensures that the proportion of interim censored observations is equal to 0.5. This is achieved by:
  - repeatedly simulated event times  $T$  conditional on  $\exp(\beta Z)$ , interim and loss to follow-up censoring times  $\mathcal{T}, L$  with NORTA sampling (bisection for  $\rho$  is then executed) and by putting  $\psi = k\lambda_0$ .

- computed the empirical proportion of censored data at the interim time  $t_c$  through the corresponding indicator.
- updated  $\lambda_0$  until this proportion matched the target within a pre-specified tolerance.

After finding the appropriate  $\lambda_0$ , the simulated data are obtained as described in the above section.

### 7.6.2 Data-generating mechanisms - $\mathcal{S}_2$

1. Fix the design values of the simulation  $\Delta t, t_c, HR, p(t_c)$ .
2. Find with the bisection procedure the value of  $\lambda_0$  that ensures that the proportion of interim censored observations is equal to  $p(t_c)$ . This is achieved by:
  - repeatedly simulated event times  $T$  conditional on  $\exp(\beta Z)$  and interim times  $\mathcal{T}$ .
  - computed the empirical proportion of censored data at the interim time  $t_c$  through the corresponding indicator.
  - updated  $\lambda_0$  until this proportion matched the target within a pre-specified tolerance.

After finding the appropriate  $\lambda_0$ , data are simulated as described in the above section.

Table 2 reports the values of  $\lambda_0$  and  $\psi$  corresponding to each combination of simulation factor levels, together with the mean upper and lower prediction bounds of the predictive distribution evaluated at the true values of  $\lambda_0, \gamma$  and  $\psi$ . Table 3 reports the values of  $\lambda_0$  for study  $\mathcal{S}_2$  (only interim censoring) corresponding to each combination of simulation factor levels, together with the mean upper and lower prediction bounds of the predictive distribution evaluated at the true values of  $\lambda_0$  and  $\gamma$ .

### 7.7 Further simulations results - $\mathcal{S}_1$

Table 2: Summary of  $\lambda$ ,  $\psi$  and true bounds by scenario.

$t_c$	$k$	HR	$t_f$	$\rho$	$\bar{\lambda}$	$\min(\lambda)$	$\max(\lambda)$	$\bar{\psi}$	$\min(\psi)$	$\max(\psi)$	$\bar{L}_{\text{true}}$	$\bar{U}_{\text{true}}$
1	1	1	0.2	0.1	0.624	0.562	0.664	0.062	0.056	0.066	50.9	79.4
1	1	1	0.2	0.5	0.624	0.562	0.664	0.062	0.056	0.066	51.8	80.5
1	1	1	0.8	0.1	0.385	0.362	0.411	0.039	0.036	0.041	60.1	91.7
1	1	1	0.8	0.5	0.385	0.362	0.411	0.039	0.036	0.041	60.9	92.7
1	1	4	0.2	0.1	0.624	0.562	0.664	0.062	0.056	0.066	144.0	182.4
1	1	4	0.2	0.5	0.624	0.562	0.664	0.062	0.056	0.066	146.1	184.7
1	1	4	0.8	0.1	0.385	0.362	0.411	0.039	0.036	0.041	184.6	229.5
1	1	4	0.8	0.5	0.385	0.362	0.411	0.039	0.036	0.041	186.6	231.7
1	2	1	0.2	0.1	0.498	0.445	0.562	0.100	0.089	0.112	48.3	76.6
1	2	1	0.2	0.5	0.498	0.445	0.562	0.100	0.089	0.112	49.4	78.0
1	2	1	0.8	0.1	0.335	0.305	0.375	0.067	0.061	0.075	56.3	87.2
1	2	1	0.8	0.5	0.335	0.305	0.375	0.067	0.061	0.075	57.4	88.7
1	2	4	0.2	0.1	0.498	0.445	0.562	0.100	0.089	0.112	134.0	172.8
1	2	4	0.2	0.5	0.498	0.445	0.562	0.100	0.089	0.112	136.3	175.4
1	2	4	0.8	0.1	0.335	0.305	0.375	0.067	0.061	0.075	169.3	214.2
1	2	4	0.8	0.5	0.335	0.305	0.375	0.067	0.061	0.075	171.8	217.0
1	3	1	0.2	0.1	0.422	0.393	0.469	0.127	0.118	0.141	44.5	72.1
1	3	1	0.2	0.5	0.422	0.393	0.469	0.127	0.118	0.141	45.4	73.2
1	3	1	0.8	0.1	0.297	0.278	0.328	0.089	0.083	0.098	52.0	82.1
1	3	1	0.8	0.5	0.297	0.278	0.328	0.089	0.083	0.098	52.9	83.4
1	3	4	0.2	0.1	0.422	0.393	0.469	0.127	0.118	0.141	121.1	159.3
1	3	4	0.2	0.5	0.422	0.393	0.469	0.127	0.118	0.141	123.0	161.5
1	3	4	0.8	0.1	0.297	0.278	0.328	0.089	0.083	0.098	153.4	197.7
1	3	4	0.8	0.5	0.297	0.278	0.328	0.089	0.083	0.098	155.7	200.4
2	1	1	0.2	0.1	0.400	0.363	0.434	0.040	0.036	0.043	26.6	49.1
2	1	1	0.2	0.5	0.400	0.363	0.434	0.040	0.036	0.043	26.9	49.6
2	1	1	0.8	0.1	0.259	0.234	0.281	0.026	0.023	0.028	31.0	55.6
2	1	1	0.8	0.5	0.259	0.234	0.281	0.026	0.023	0.028	31.4	56.1
2	1	4	0.2	0.1	0.400	0.363	0.434	0.040	0.036	0.043	93.1	127.7
2	1	4	0.2	0.5	0.400	0.363	0.434	0.040	0.036	0.043	94.1	128.8
2	1	4	0.8	0.1	0.259	0.234	0.281	0.026	0.023	0.028	114.3	154.0
2	1	4	0.8	0.5	0.259	0.234	0.281	0.026	0.023	0.028	115.6	155.5
2	2	1	0.2	0.1	0.311	0.281	0.334	0.062	0.056	0.067	23.9	45.9
2	2	1	0.2	0.5	0.311	0.281	0.334	0.062	0.056	0.067	24.4	46.4
2	2	1	0.8	0.1	0.219	0.205	0.240	0.044	0.041	0.048	28.5	52.4
2	2	1	0.8	0.5	0.219	0.205	0.240	0.044	0.041	0.048	28.7	52.8
2	2	4	0.2	0.1	0.311	0.281	0.334	0.062	0.056	0.067	82.7	116.6
2	2	4	0.2	0.5	0.311	0.281	0.334	0.062	0.056	0.067	83.9	118.0
2	2	4	0.8	0.1	0.219	0.205	0.240	0.044	0.041	0.048	103.2	142.1
2	2	4	0.8	0.5	0.219	0.205	0.240	0.044	0.041	0.048	104.0	143.0
2	3	1	0.2	0.1	0.258	0.234	0.281	0.077	0.070	0.084	21.3	42.4
2	3	1	0.2	0.5	0.258	0.234	0.281	0.077	0.070	0.084	21.6	42.9
2	3	1	0.8	0.1	0.191	0.176	0.211	0.057	0.053	0.063	25.6	48.6
2	3	1	0.8	0.5	0.191	0.176	0.211	0.057	0.053	0.063	25.9	49.0
2	3	4	0.2	0.1	0.258	0.234	0.281	0.077	0.070	0.084	72.8	105.6
2	3	4	0.2	0.5	0.258	0.234	0.281	0.077	0.070	0.084	73.6	106.6
2	3	4	0.8	0.1	0.191	0.176	0.211	0.057	0.053	0.063	91.3	128.8
2	3	4	0.8	0.5	0.191	0.176	0.211	0.057	0.053	0.063	92.2	129.8
4	1	1	0.2	0.1	0.306	0.278	0.331	0.031	0.028	0.033	17.2	36.6
4	1	1	0.2	0.5	0.306	0.278	0.331	0.031	0.028	0.033	17.4	36.7
4	1	1	0.8	0.1	0.202	0.187	0.217	0.020	0.019	0.022	20.2	41.1
4	1	1	0.8	0.5	0.202	0.187	0.217	0.020	0.019	0.022	20.4	41.4
4	1	4	0.2	0.1	0.306	0.278	0.331	0.031	0.028	0.033	67.8	99.3
4	1	4	0.2	0.5	0.306	0.278	0.331	0.031	0.028	0.033	68.3	99.8
4	1	4	0.8	0.1	0.202	0.187	0.217	0.020	0.019	0.022	82.5	118.1
4	1	4	0.8	0.5	0.202	0.187	0.217	0.020	0.019	0.022	83.0	118.7
4	2	1	0.2	0.1	0.233	0.211	0.259	0.047	0.042	0.052	15.1	33.6
4	2	1	0.2	0.5	0.233	0.211	0.259	0.047	0.042	0.052	15.4	34.0
4	2	1	0.8	0.1	0.168	0.152	0.188	0.034	0.030	0.038	18.3	38.4
4	2	1	0.8	0.5	0.168	0.152	0.188	0.034	0.030	0.038	18.5	38.6
4	2	4	0.2	0.1	0.233	0.211	0.259	0.047	0.042	0.052	59.0	89.5
4	2	4	0.2	0.5	0.233	0.211	0.259	0.047	0.042	0.052	59.8	90.4
4	2	4	0.8	0.1	0.168	0.152	0.188	0.034	0.030	0.038	73.4	107.8
4	2	4	0.8	0.5	0.168	0.152	0.188	0.034	0.030	0.038	73.8	108.3
4	3	1	0.2	0.1	0.189	0.175	0.200	0.057	0.053	0.060	12.7	30.1
4	3	1	0.2	0.5	0.189	0.175	0.200	0.057	0.053	0.060	13.0	30.6
4	3	1	0.8	0.1	0.144	0.135	0.164	0.043	0.040	0.049	15.7	34.8
4	3	1	0.8	0.5	0.144	0.135	0.164	0.043	0.040	0.049	15.9	35.0
4	3	4	0.2	0.1	0.189	0.175	0.200	0.057	0.053	0.060	49.6	78.4
4	3	4	0.2	0.5	0.189	0.175	0.200	0.057	0.053	0.060	50.5	79.4
4	3	4	0.8	0.1	0.144	0.135	0.164	0.043	0.040	0.049	62.7	95.3
4	3	4	0.8	0.5	0.144	0.135	0.164	0.043	0.040	0.049	63.2	95.9

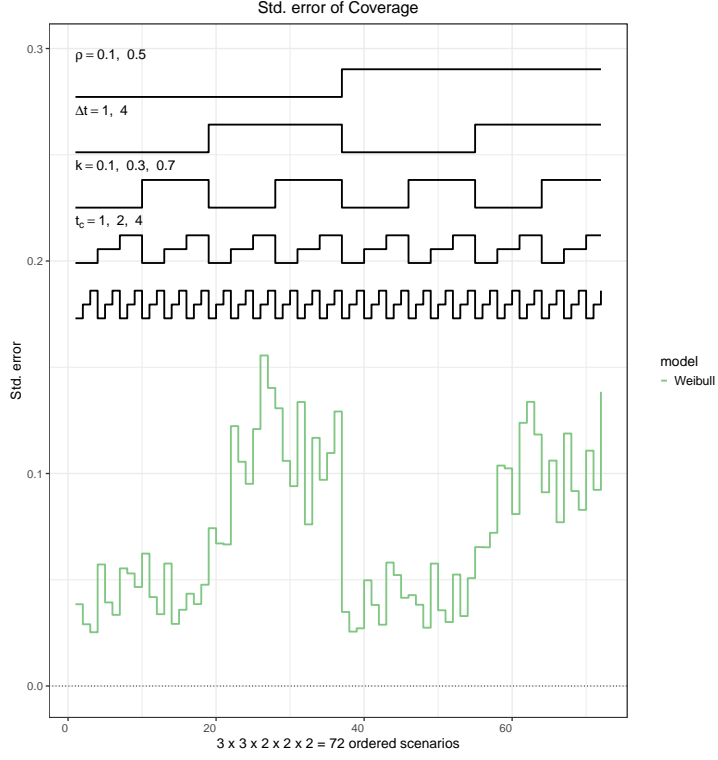


Figure 5: Standard errors of the coverage.

## 7.8 Further simulations results - $\mathcal{S}_2$

Table 3: Summary of  $\lambda_0$  and true bounds by scenario.

$t_c$	Censoring	HR	$t_f$	$\bar{\lambda}_0$	$\min(\lambda_0)$	$\max(\lambda_0)$	$\bar{L}_{\text{true}}$	$\bar{U}_{\text{true}}$
1	0.2	0.2	1	2.816	2.438	2.991	34.0	56.6
1	0.2	0.2	4	2.815	2.531	2.989	99.0	126.2
1	0.2	0.8	1	1.103	1.019	1.219	53.3	79.2
1	0.2	0.8	4	1.103	1.008	1.219	135.7	159.7
1	0.8	0.2	1	0.233	0.188	0.281	27.4	50.8
1	0.8	0.2	4	0.232	0.187	0.281	101.7	139.5
1	0.8	0.8	1	0.146	0.123	0.167	29.2	53.6
1	0.8	0.8	4	0.146	0.117	0.170	111.0	152.0
2	0.2	0.2	1	1.927	1.687	2.250	16.5	34.6
2	0.2	0.2	4	1.929	1.687	2.250	61.7	88.1
2	0.2	0.8	1	0.745	0.656	0.803	27.6	49.2
2	0.2	0.8	4	0.746	0.680	0.820	92.7	120.2
2	0.8	0.2	1	0.161	0.129	0.188	13.1	30.9
2	0.8	0.2	4	0.160	0.135	0.189	58.5	89.7
2	0.8	0.8	1	0.101	0.088	0.119	14.1	32.5
2	0.8	0.8	4	0.102	0.088	0.118	63.5	96.6
4	0.2	0.2	1	1.538	1.359	1.875	10.3	25.7
4	0.2	0.2	4	1.537	1.312	1.875	44.9	69.5
4	0.2	0.8	1	0.592	0.551	0.633	18.0	36.8
4	0.2	0.8	4	0.592	0.539	0.656	69.6	96.7
4	0.8	0.2	1	0.129	0.105	0.152	8.1	23.0
4	0.8	0.2	4	0.129	0.105	0.152	40.6	67.9
4	0.8	0.8	1	0.081	0.067	0.094	8.7	24.2
4	0.8	0.8	4	0.081	0.069	0.094	43.8	72.4

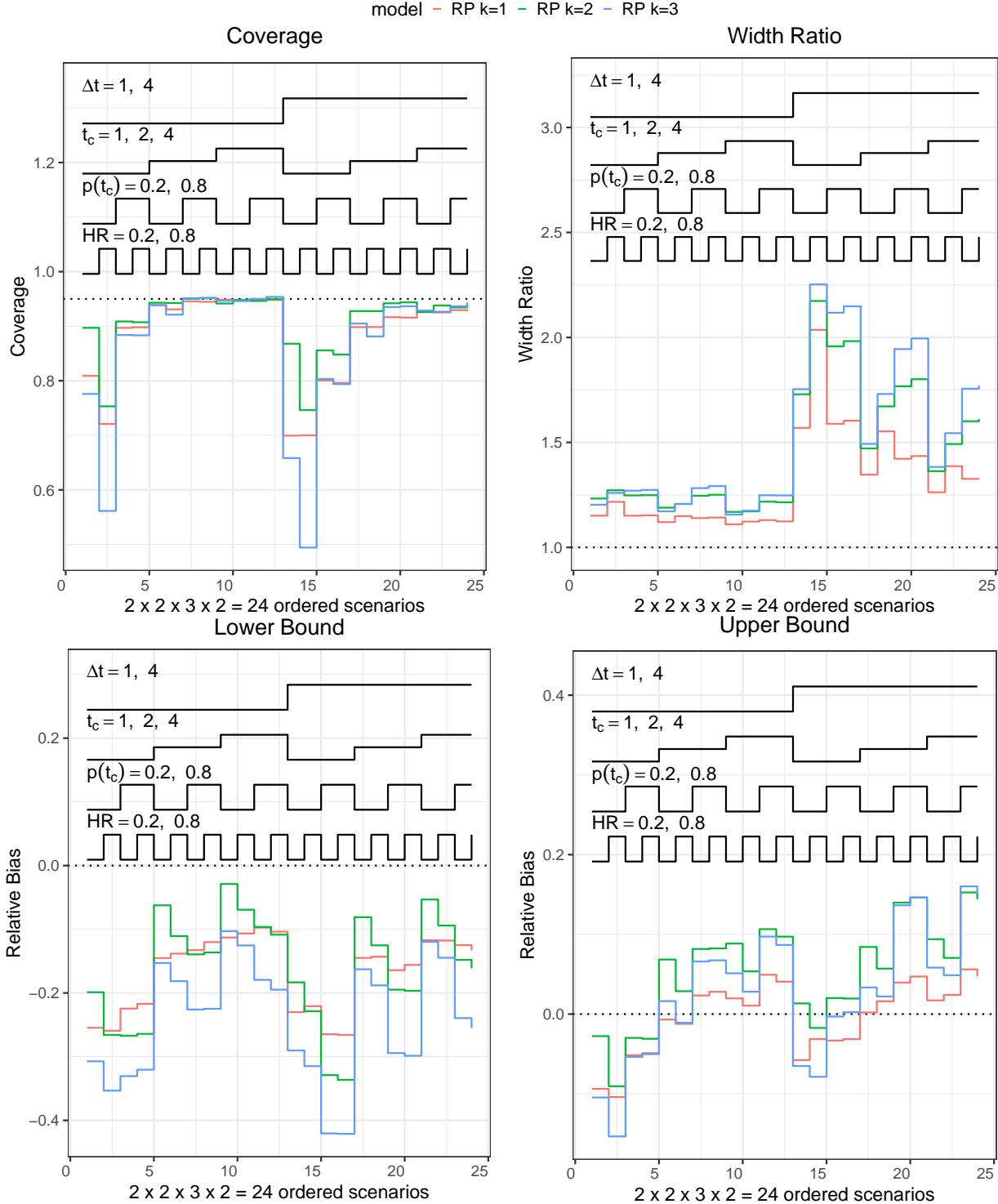


Figure 6: Coverage probability of the 95% two-sided prediction intervals under different models and administrative censoring only at  $t_c$ .  $p(t_c)$  denotes the proportion of interim censored patients,  $\Delta t$  denotes the prediction horizon,  $t_c$  the time of interim from accrual end,  $HR$  is the hazard ratio and  $k$  the ratio between the baseline event rate and the loss to follow-up rate. RP = Royston - Parmar,  $k$  denotes the number of knots.

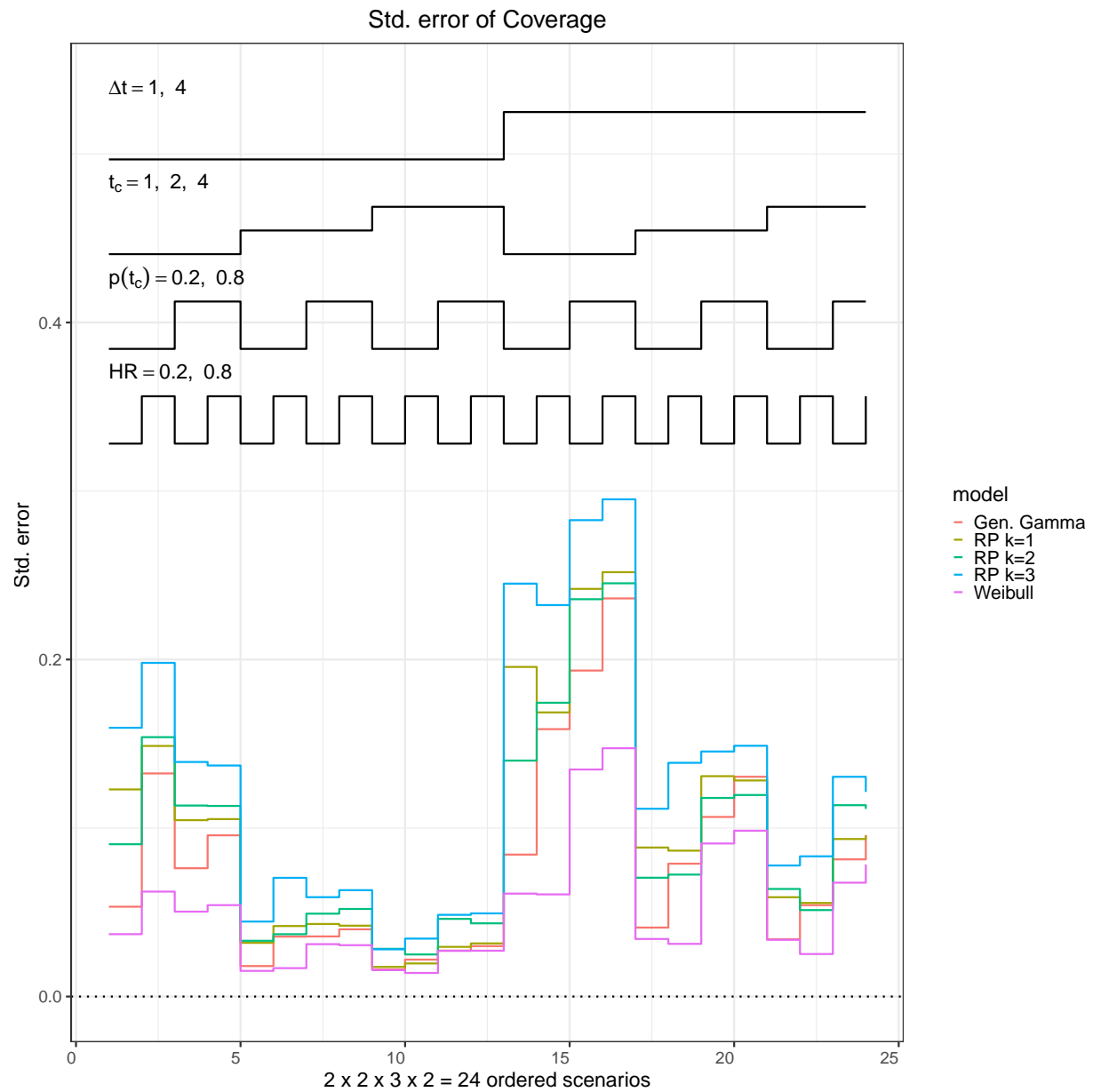


Figure 7: Standard errors of the coverage.

## 7.9 Further case study results

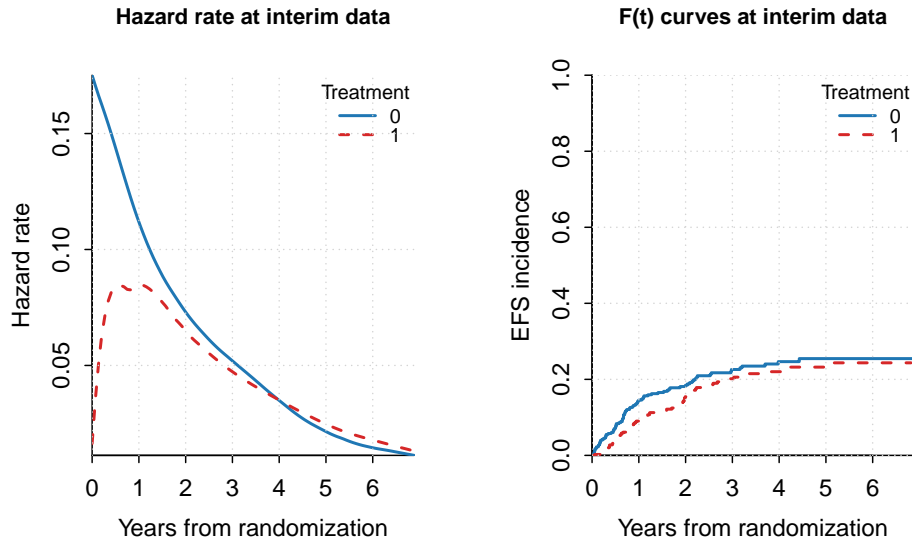


Figure 8: Smoothed hazard function and Incidence function for event survival probability (EFS) at 1-06-2017. 1 = Active treatment, 0 = standard of care.

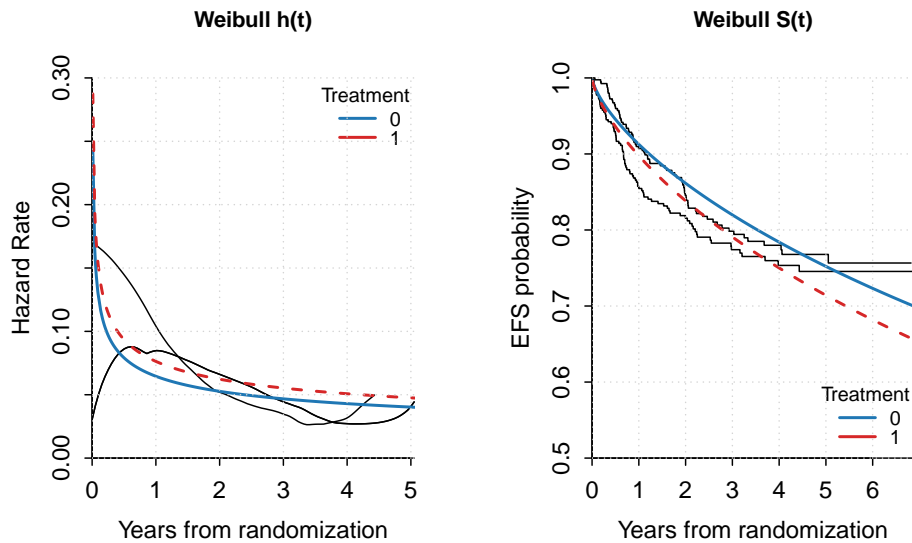


Figure 9: Observed vs predicted hazard curves (left) and survival curves (right) under Weibull models at 1-06-2017. Solid lines refer to active treatment, dashed lines to standard of care.

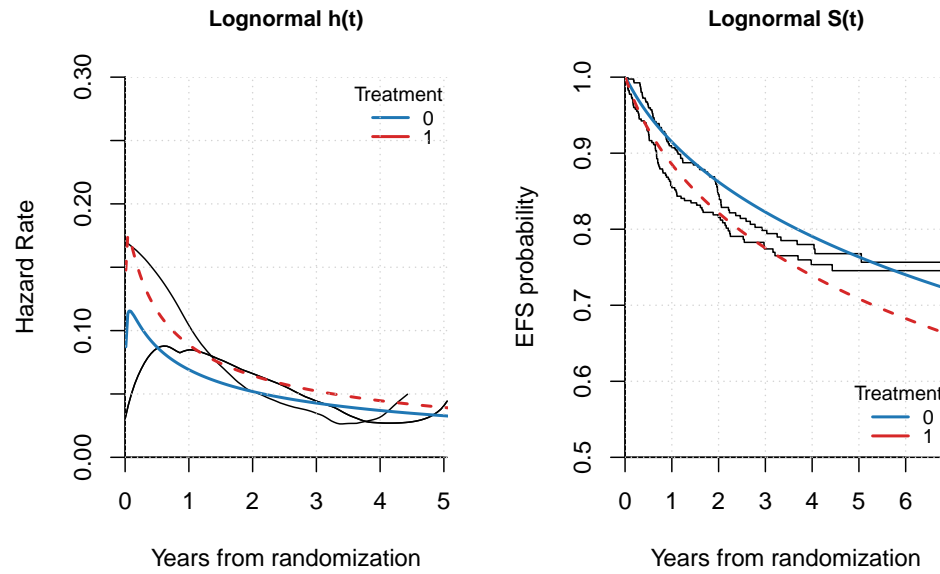


Figure 10: Observed vs predicted hazard curves (left) and survival curves (right) under Lognormal models at 1-06-2017. Solid lines refer to active treatment, dashed lines to standard of care.

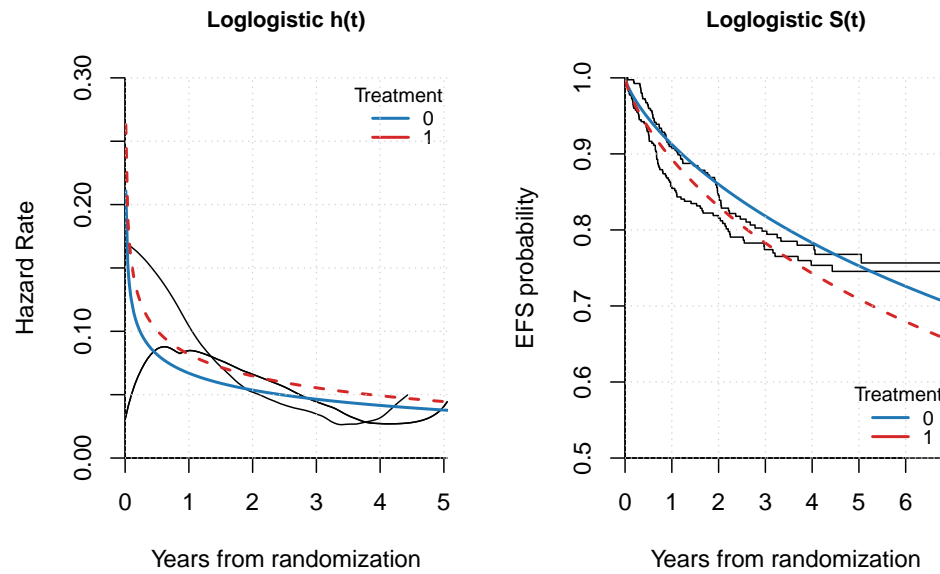


Figure 11: Observed vs predicted hazard curves (left) and survival curves (right) under Loglogistic models at 1-06-2017. Solid lines refer to active treatment, dashed lines to standard of care.

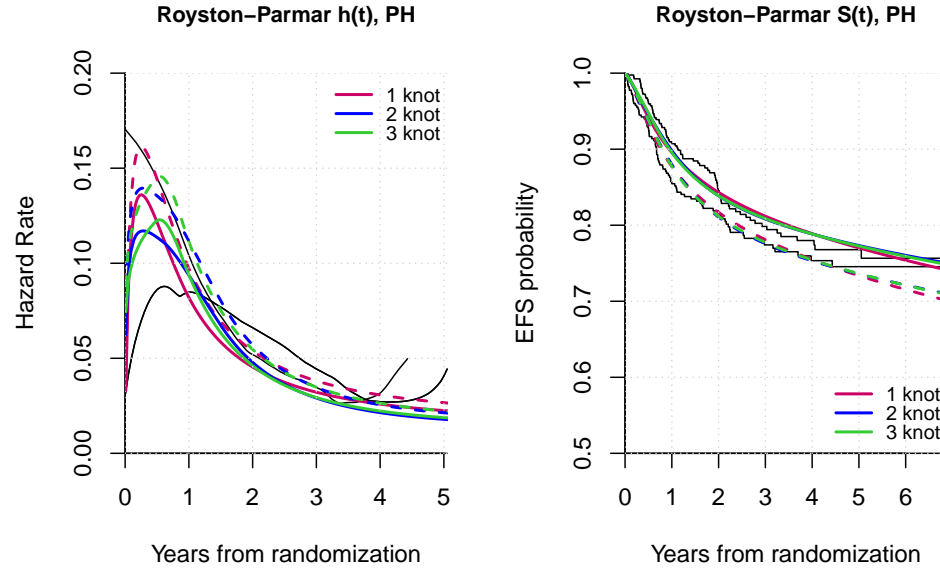


Figure 12: Observed vs predicted hazard curves (left) and survival curves (right) under Royston-Parmar models on the proportional hazard scale at 1-06-2017. Solid lines refer to active treatment, dashed lines to standard of care.

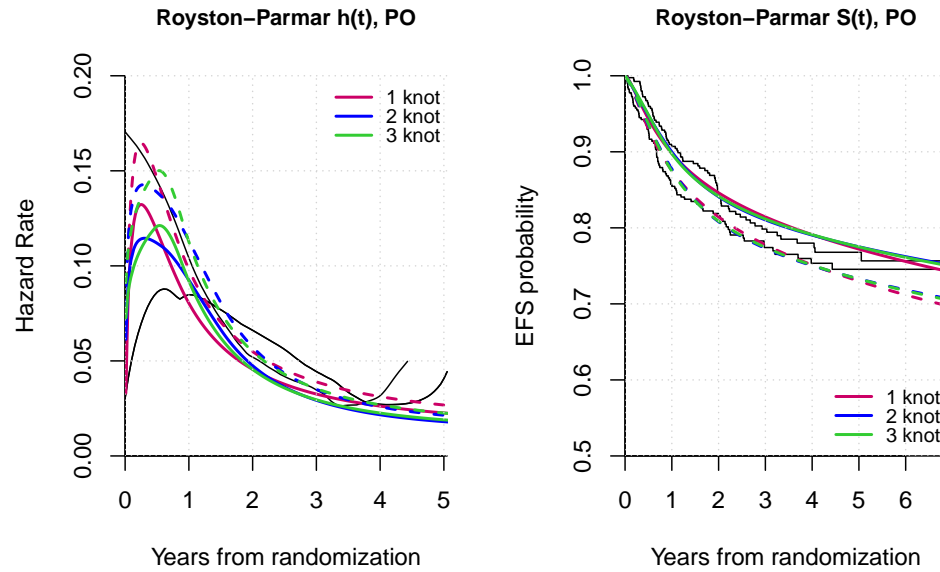


Figure 13: Observed vs predicted hazard curves (left) and survival curves (right) under Royston-Parmar models on the proportional odds scale at 1-06-2017. Solid lines refer to active treatment, dashed lines to standard of care.

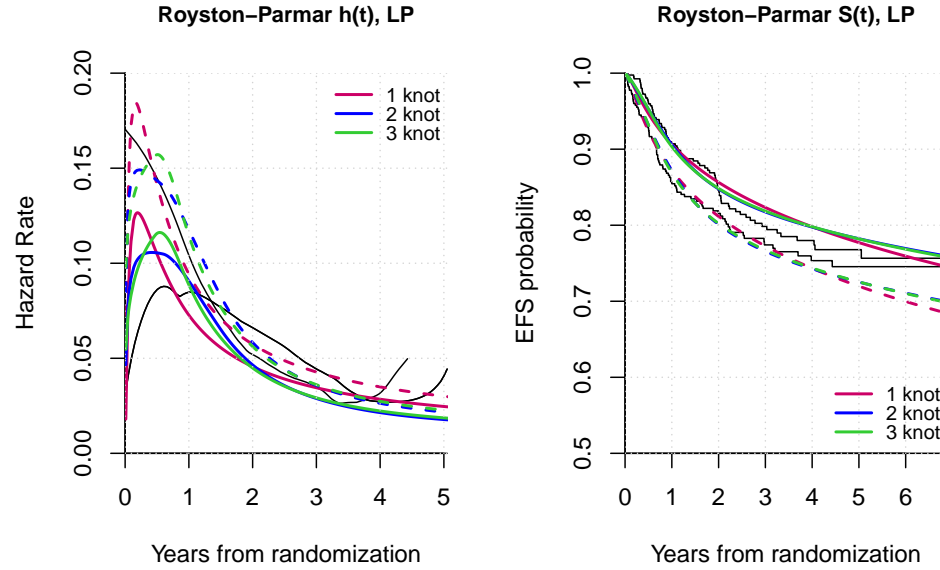


Figure 14: Observed vs predicted hazard curves (left) and survival curves (right) under Royston-Parmar models on the linear probit scale at 1-06-2017. Solid lines refer to active treatment, dashed lines to standard of care.

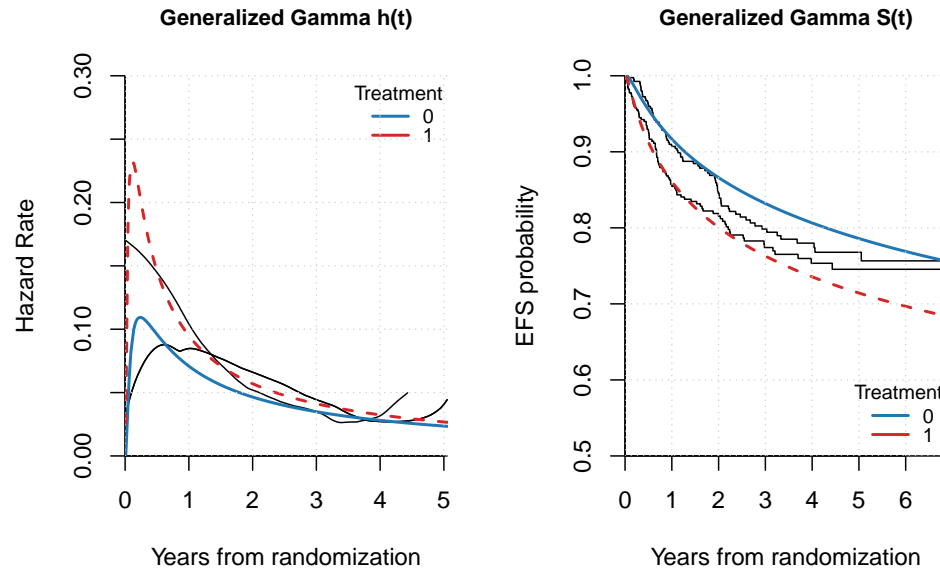


Figure 15: Observed vs predicted hazard curves (left) and survival curves (right) under Generalized Gamma models at 1-06-2017. Solid lines refer to active treatment, dashed lines to standard of care.

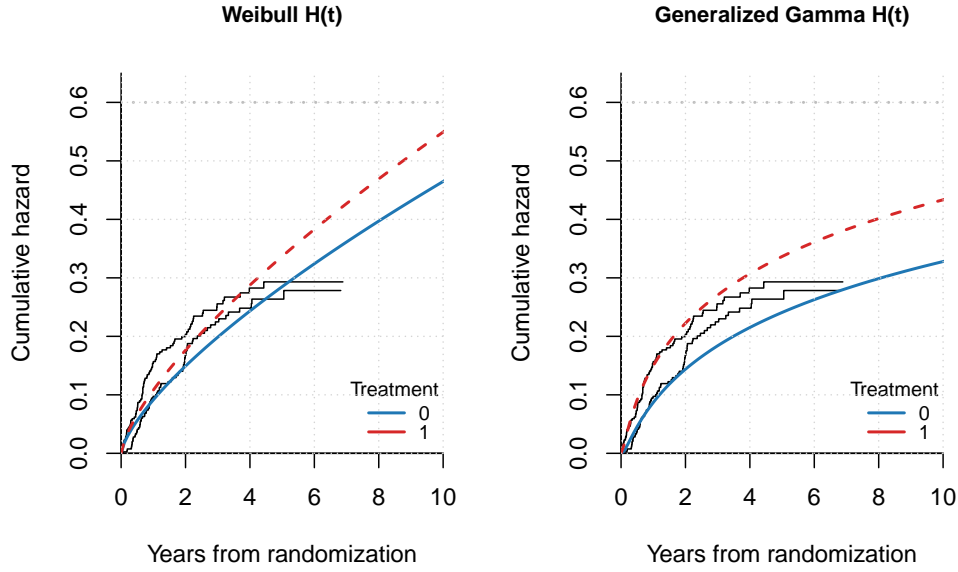


Figure 16: Observed vs predicted cumulative hazard curves under the Weibull and the Generalized Gamma model at 1-06-2017. Solid lines refer to active treatment, dashed lines to standard of care. A grey dashed line is added for reference in comparing the plots

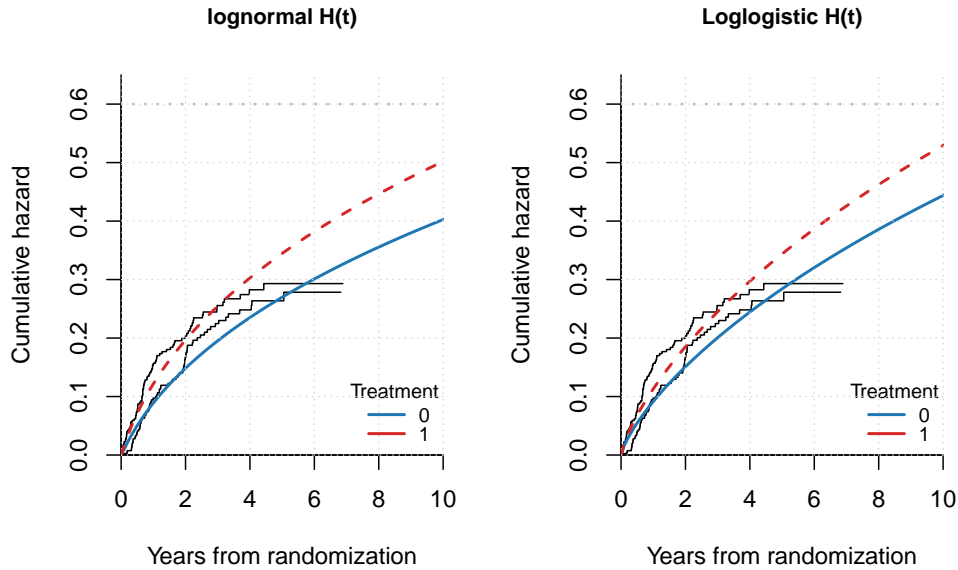


Figure 17: Observed vs predicted cumulative hazard curves under the Lognormal and the Loglogistic model at 1-06-2017. Solid lines refer to active treatment, dashed lines to standard of care. A grey dashed line is added for reference in comparing the plots

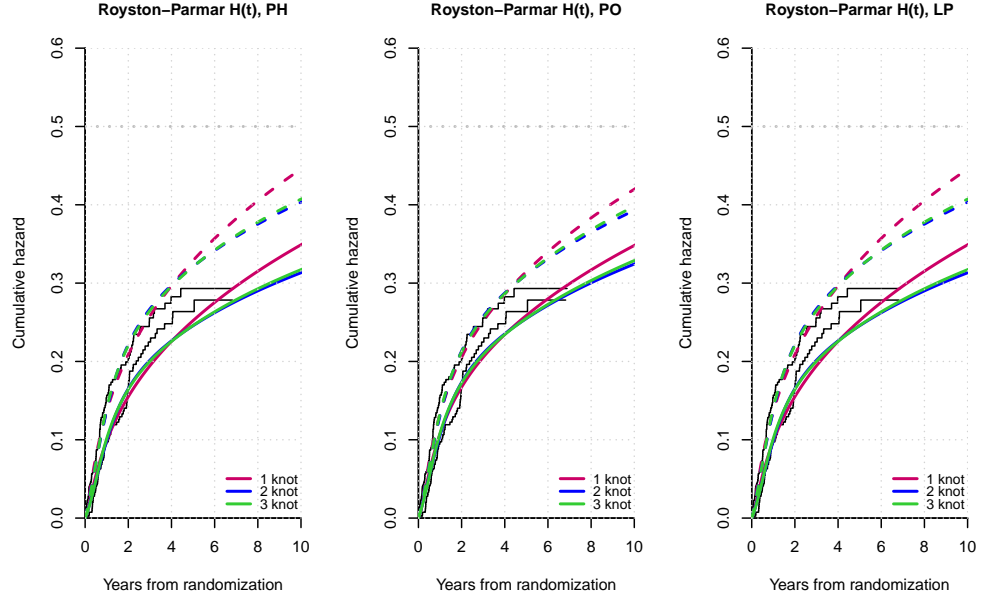


Figure 18: Observed vs predicted cumulative hazard curves under the Royston - Parmar model at 1-06-2017. Solid lines refer to active treatment, dashed lines to standard of care. PH = proportional hazard, PO = proportional odds, LP = linear probit. A grey dashed line is added for reference in comparing the plots

Table 4: Prediction intervals (lower, upper) for additional events

Date	Additional Events	Weibull	RP, 1 knot	RP, 2 knots	RP, 3 knots	GG
1/12/2017	17	(7, 22)	(6, 21)	(6, 21)	(6, 21)	(6, 21)
1/06/2018	29	(19, 40)	(13, 34)	(13, 33)	(13, 33)	(13, 34)
1/12/2018	43	(28, 57)	(19, 45)	(18, 43)	(18, 44)	(20, 45)
1/06/2019	50	(38, 70)	(25, 54)	(23, 52)	(22, 53)	(26, 54)
1/12/2019	53	(49, 84)	(30, 63)	(26, 60)	(26, 61)	(31, 63)
1/06/2020	55	(58, 97)	(34, 71)	(30, 67)	(29, 70)	(36, 70)
1/12/2020	60	(67, 111)	(38, 79)	(33, 74)	(32, 77)	(41, 77)
1/06/2021	62	(74, 123)	(42, 86)	(35, 81)	(34, 85)	(45, 84)

Note: RP = Royston-Parmar model; GG = Generalized Gamma model.

Table 5: Prediction intervals (lower, upper) for additional events — Lognormal and Royston-Parmar extensions

Date	Additional Events	Lognormal	RP, 1 knot	RP, 2 knots	RP, 3 knots
1/12/2017	17	(8, 24)	(6, 22)	(6, 21)	(6, 21)
1/06/2018	29	(17, 40)	(14, 35)	(13, 33)	(13, 33)
1/12/2018	43	(27, 54)	(21, 46)	(18, 43)	(18, 44)
1/06/2019	50	(36, 66)	(27, 57)	(23, 52)	(23, 53)
1/12/2019	53	(44, 78)	(33, 66)	(27, 60)	(27, 61)
1/06/2020	55	(51, 88)	(38, 74)	(30, 67)	(39, 69)
1/12/2020	60	(59, 98)	(43, 82)	(33, 73)	(34, 77)
1/06/2021	62	(65, 108)	(48, 90)	(36, 80)	(36, 84)

Note: RP = Royston-Parmar model.

Table 6: Prediction intervals (lower, upper) for additional events — Loglogistic and Royston–Parmar extensions

Date	Additional Events	Loglogistic	RP, 1 knot	RP, 2 knots	RP, 3 knots
1/12/2017	17	(8, 24)	(7, 23)	(7, 22)	(7, 23)
1/06/2018	29	(18, 41)	(15, 37)	(14, 36)	(14, 36)
1/12/2018	43	(28, 56)	(22, 48)	(20, 47)	(20, 47)
1/06/2019	50	(38, 70)	(28, 59)	(25, 56)	(25, 57)
1/12/2019	53	(47, 83)	(33, 68)	(29, 65)	(28, 66)
1/06/2020	55	(55, 95)	(38, 76)	(32, 72)	(32, 75)
1/12/2020	60	(63, 106)	(42, 84)	(36, 80)	(35, 83)
1/06/2021	62	(71, 117)	(46, 92)	(38, 86)	(37, 90)

*Note:* RP = Royston–Parmar model.